



Giovanni Polese

THE DETECTOR CONTROL SYSTEMS FOR THE CMS RESISTIVE PLATE CHAMBER AT LHC

*Thesis for the degree of Doctor of Philosophy to be presented
for public examination and criticism in the Auditorium 1381
at Lappeenranta University of Technology, Lappeenranta,
Finland, on the 3rd of December, 2009, at noon.*

- Supervisor Professor Tuure Tuuva
Department of Mathematics and Physics
Lappeenranta University of Technology
Finland
- Reviewers Dr. Hartmut F.-W. Sadrozinski
Professor, Physics Department
University of California
Santa Cruz, USA
- Dr. Martti Voutilainen
Nokia Research Center
Finland
- Opponents Dr. Paula Eerola
Professor at the Division of Elementary Particle Physics
University of Helsinki, Helsinki
Finland

ISBN 978-952-214-855-1
ISBN 978-952-214-856-8 (PDF)
ISSN 1456-4491
Lappeenrannan teknillinen yliopisto
Digipaino 2009

ABSTRACT

Giovanni Polese

The Detector Control Systems for the CMS Resistive Plate Chamber at LHC

Acta Universitatis Lappeenrantaensis 365

Diss. Lappeenranta University of Technology 2009

ISBN 978-952-214-855-1 ISBN 978-952-214-856-8 (PDF) ISSN 1456-4491

97 pages.

The RPC Detector Control System (RCS) is the main subject of this PhD work. The project, involving the Lappeenranta University of Technology, the Warsaw University and INFN of Naples, is aimed to integrate the different subsystems for the RPC detector and its trigger chain in order to develop a common framework to control and monitoring the different parts. In this project, I have been strongly involved during the last three years on the hardware and software development, construction and commissioning as main responsible and coordinator.

The CMS Resistive Plate Chambers (RPC) system consists of 912 double-gap chambers at its start-up in middle of 2008. A continuous control and monitoring of the detector, the trigger and all the ancillary sub-systems (high voltages, low voltages, environmental, gas, and cooling), is required to achieve the operational stability and reliability of a so large and complex detector and trigger system. Role of the RPC Detector Control System is to monitor the detector conditions and performance, control and monitor all subsystems related to RPC and their electronics and store all the information in a dedicated database, called Condition DB. Therefore the RPC DCS system has to assure the safe and correct operation of the sub-detectors during all CMS life time (more than 10 year), detect abnormal and harmful situations and take protective and automatic actions to minimize consequential damages.

The analysis of the requirements and project challenges, the architecture design and its development as well as the calibration and commissioning phases represent the main tasks of the work developed for this PhD thesis. Different technologies, middleware and solutions has been studied and adopted in the design and development of the different components and a big challenging consisted in the integration of these different parts each other and in the general CMS control system and data acquisition framework.

Therefore, the RCS installation and commissioning phase as well as its performance and the first results, obtained during the last three years CMS cosmic runs, will be described in this thesis.

Keywords: CMS, DAQ, Detector Control System, Resistive Plate Chambers.

UDC 681.5.08 : 539.1.074

List of Publications

- Publication I** *Paolucci P. and Polese G. , “The Detector Control Systems for the CMS Resistive Plate Chamber”, “CMS-NOTE-2008-036. CERN-CMS-NOTE-2008-036”*
- Publication II** *Colaleo A. et al, “First Measurements of the Performance of the Barrel RPC System in CMS”, Nuclear Instruments and Methods in Physics Research Section A: Accelerators, Spectrometers, Detectors and Associated Equipment, Volume 609, Issues 2-3, Pages 114-121*
- Publication III** *Paolucci P. et al, “The compact muon solenoid RPC barrel detector” Nuclear Instruments and Methods in Physics Research A602(2009)674-678.*
- Publication IV** *Polese G. et al, “The Detector Control Systems for the CMS Resistive Plate Chamber at LHC”, J. Phys.: Conf. Ser. CHEP09 Proceeding in press. Also CMS-CR-2009-136.*
- Publication V** *Guida R. et al, “The gas monitoring system for the resistive plate chamber detector of the CMS experiment at LHC”. Nuclear Physics B (Proc. Suppl.) 177-178 (2008) 293-296*

Author's Contribution

The author has contributed actively to the work described in all these publications by doing software development and hardware commissioning and testing. Part of the main result of his work during the PhD are described in Publication I and IV, of which he is the correspondent author. They dealt with the RPC DCS, project started from scratch by the author whose he is the main designer, developer, and responsible person for the CMS RPC community. The results of these publications have been also presented by the author at IEEE 2008 and at CHEP09 international conferences. Publications II, III, and V are written together with the RPC Collaboration as result of commissioning phase, where the first results of the Detector control and power supply system, developed during the thesis by the author, are described.

Summary of Publications

Publication I represents the first publication in the RPC Community where the RPC Detector Control System is described. The mission and requirements of such system as well the challenges in the design and development are described, underlying the particular solutions adopted in the different scenarios.

Publication II describes the first results obtained by the RPC detector during the first integrated test of a part of the CMS experiment performed at CERN in autumn 2006. Here all the RPC subsystems involved in the RPC operation are described, e.g. DAQ, DCS and DQM as well as their performances.

Publication III briefly summarizes the installation and commissioning period, illustrating the challenges and the problematic encountered during it and the solutions adopted in the system optimization. A large section of the power supply system and its performance is here presented where the author has been deeply involved in the design, installation and testing.

Publication IV illustrates the state of art of the RPC DCS. It summarizes the first years of RPC DCS activities, describing its evolution and peculiarities. The technical solutions and the design choices implemented by the author for the different specific tasks are described and the key points are pointed out. For each subsystem involved in the RPC DCS is

also presented the characteristics and the performances during these two years and the integration process inside the central CMS DCS.

Publication V describes the RPC gas system monitoring. It illustrates the mission and the challenges for operating the RPC detector in the CMS environment. An overview of both the CMS-RPC gas system and gas monitoring system is given and its integration in the RPC DCS.

CONTENTS

Abstract	2
List of Publications	4
Author's Contribution	5
Summary of Publications	5
1 THE CMS EXPERIMENT	13
1.1 The Large Hadron Collider	13
1.2 The LHC Physics goals	15
1.3 The CMS detector	16
1.3.1 Requirements	19
1.3.2 The Tracking system	19
1.3.3 The Calorimeters	21
1.3.4 The Magnet	25
1.3.5 The Muon System	25

1.4	The CMS Online Trigger and Data Acquisition (TriDAS)	29
1.4.1	The Level 1 Trigger	30
1.4.2	The High Level Trigger	31
2	THE CMS EXPERIMENT CONTROL SYSTEM	33
2.1	Data Acquisition System (DAQ)	33
2.1.1	Cross-platform DAQ framework	35
2.2	Run Control and Monitoring System	36
2.2.1	Architecture and Functionalities	37
2.2.2	Software Components	39
2.3	Detector Control System	39
2.3.1	Mission and Requirements	40
2.3.2	Architecture and Functionalities	40
2.3.3	Software Framework	42
3	THE RPC DETECTOR CONTROL SYSTEM	47
3.1	Mission and Requirements	48
3.2	The CMS RPC Detector	48
3.2.1	Design Requirements	49
3.2.2	Detector Layout	49
3.2.3	Read-out electronics	52

3.3	The RCS Architecture	54
3.4	The RPC Power Supply System	55
3.4.1	The DCS of the Power System	57
3.5	The Environmental Control System	59
3.5.1	The DCS of the Environmental Control System	60
3.6	The Gas System Monitoring	62
3.6.1	The Gas monitoring Applications	64
3.7	External Control System	65
3.7.1	Cooling and Ventilation	65
3.7.2	Detector Safety System	66
3.8	The RCS Supervisor	67
3.8.1	Architecture	67
3.8.2	The Finite State Machine	68
3.8.3	The Graphical User Interface (GUI)	70
3.8.4	Alert Handling	71
3.8.5	Integration in central DCS and Run Control	72
3.8.6	DCS Configuration	72
3.8.7	Condition Database	74
4	THE COMMISSIONING AND CALIBRATION	75
4.1	CMS Global data taking	75

4.2	RPC Performance and Calibration	77
4.2.1	RPC working point calibration	79
4.3	The RCS performance during the CMS global runs	82
4.3.1	RPC Detector Performance analysis tool for not event data	83
4.3.2	Power System performances	83
4.3.3	Temperature	85
4.3.4	DCS performances	87
5	CONCLUSIONS	89
	REFERENCES	92

ABBREVIATIONS

ALICE	A Large Ion Collider Experiment at the LHC
ATLAS	A Toroidal LHC ApparatuS experiment
CERN	Centre Européen pour la Recherche Nucléaire
CMS	Compact Muon Solenoid experiment
CRAFT	Cosmic Run At Four Tesla
CSC	Cathode Strip Chambers
DAQ	Data Acquisition System
DCS	Detector Control System
DIM	Distributed Information Management System
DIP	Data Interchange Protocol
DQM	Data quality monitor
DSS	Detector Safety System
DT	Drift Tube
ECAL	Electromagnetic Calorimeter
ECS	Experiment Control System
FEB	Front End Board
FED	Front-End Drivers
FSM	Final State Machine
GCS	Gas Control System
HCAL	Hadronic Calorimeter
HV	High Voltage
L1T	Level 1 Trigger
LAN	Local Area Network
LB	Link Board
LHC	Large Hadron Collider
LHCB	Large Hadron Collider Beauty experiment
LINAC	LINear ACcelerator
LV	Low Voltage
MTCC	Magnet test and Cosmic Challenge
OMDS	Online Master Data Storage

OSWI	Online Software Infrastructure
OPC	OLE for Process Control
PLC	Programmable Logic Controllers
PS	Proton Synchrotron
PSX	PVSS SOAP interface
PVSS	Prozessvisualisierungssoftware
QCD	Quantum chromodynamics
QGP	Quark Gluon Plasma
RCMS	Run Control and Monitor System
RCS	RPC Control System
RPC	Resistive Plate Chamber
SMI	State Management Interface
SPS	Super Proton Synchrotron
TTC	Timing, Trigger and Control
WBM	Web Based Monitoring
WSDL	Web Service Description Language
XDAQ	Cross-Platform DAQ Framework

Chapter 1

THE CMS EXPERIMENT

1.1 The Large Hadron Collider

The Large Hadron Collider (LHC) [1] is the larger and most powerful collider ever built and will provide extraordinary opportunities in high energy particle physics thanks to its unprecedented collision energy and luminosity. In fact it will accelerate two counter-rotating beams of protons, delivered by the Super Proton Synchrotron (SPS), that will collide at 14 TeV center mass energy every 25 ns at the design luminosity of $10^{34}\text{cm}^{-1}\text{s}^{-2}$. It will operate mainly in proton-proton mode but will also collide lead nuclei to study heavy ion collisions. Collisions will take place at four interaction points where detectors (ATLAS [2], ALICE [3], CMS [4], and LHCb [5]) are located, as shown in Fig. 1.1. ATLAS and CMS are general purpose experiments designed for new physics searches and precision measurements, LHCb is a B physics and CP violation dedicated detector while ALICE is a heavy ion experiment which will study the behaviour of nuclear matter at very high energy densities.

In the first beam production stage, the protons are accelerated in a linear accelerator (LINAC) before being passed to the Proton Synchrotron (PS) for further boosting. The beams enter then the Super Proton Synchrotron (SPS) where the protons gain an energy of 450 GeV. Finally, the particles are injected into the LHC tunnel, which has a circumference of 26.7 km, where the nominal energy of each proton beam is 7 TeV and at a peak luminosity of $10^{34}\text{cm}^{-1}\text{s}^{-2}$, aiming at an annual integrated luminosity of $\sim 100\text{fb}^{-1}$. The machine parameters relevant for the operation of CMS are listed in Table 1.1. The beams

		pp	HI	
Energy per nucleon	E	7	2.76	TeV
Dipole field at 7 TeV	B	8.33	8.33	T
Design Luminosity	L	10^{34}	10^{27}	$\text{cm}^{-2} \text{s}^{-1}$
Bunch separation		25	100	ns
No of bunches	k_B	2808	592	
No. particles per bunch	N_p	1.5×10^{11}	7×10^7	

Table 1.1. The machine parameters relevant for the LHC detectors.

follow circular trajectories inside the tunnel thanks to the field generated by superconducting magnets. Each beam line consist of 1,232 superconducting dipole bending magnets generating a magnetic field of 8.36 Tesla. To accelerate the protons in opposite directions, two separated vacuum beam lines are used. At the running luminosity of $10^{34} \text{cm}^{-2} \text{s}^{-2}$, a number of 27 interaction per bunch crossing will be produced, thus the total number of proton-proton interactions will be of about 10^9 per second, allowing studies of physics processes with very small cross sections.

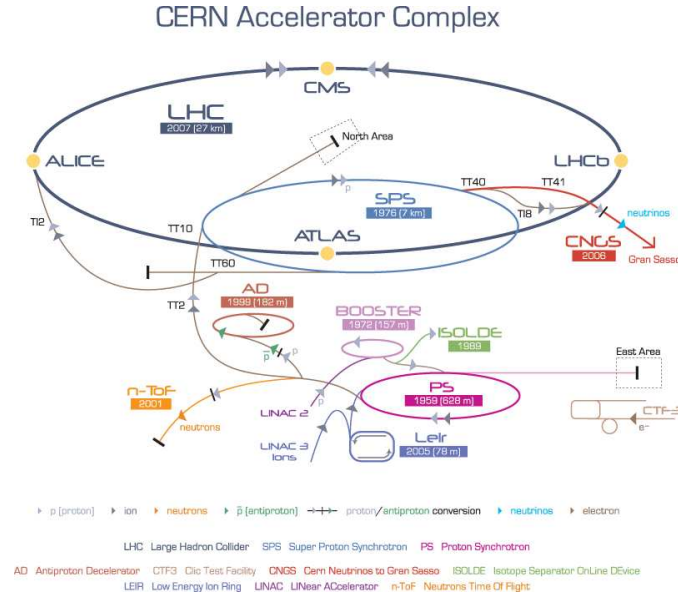


Figure 1.1. Schematic view of the LHC and the SPS accelerator ring, where the different interactions points and the corresponding detectors are shown [1].

1.2 The LHC Physics goals

The prime goals of LHC are to explore physics at the TeV scale and to study the mechanism of electroweak symmetry breaking-through for which the Higgs boson, predicted by the Standard Model (SM), is presumed to be responsible. The quest for the Higgs boson, the desire to investigate the limits of the Standard Model and its possible extensions and the study of the Quark Gluon Plasma (QGP) are the main unsolved questions of the modern physics and LHC, thanks to the energy scale reachable, will be able to provide a fundamental contributes in the understanding of these processes.

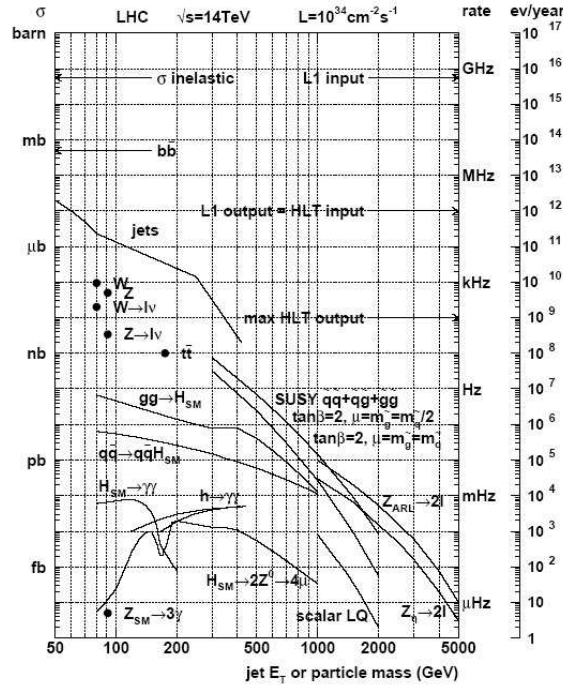


Figure 1.2. Inclusive $p - p$ cross section and corresponding interaction rates at the LHC design luminosity for selected physics processes [17].

In the design phase of CMS and ATLAS, the detection of the SM Higgs boson was used as a benchmark to test the performance of the proposed designs. It is a particularly appropriate benchmark since there is a wide range of decay modes depending on the mass of the Higgs boson. All existing direct searches and precision measurements performed at LEP and SLD are compatible with the existence of a SM-like Higgs boson of mass

between $114.4 \text{ GeV}/c^2$ and $251 \text{ GeV}/c^2$ at the 95% C.L. [6] [7], with the exclusion of the region $160\text{-}170 \text{ GeV}/c^2$ with 95% C.L. from Tevatron experiments [8]. Since in the vicinity of this limit the branching fractions of the Higgs boson are dominated by hadronic decays, difficult to detect due to the large QCD backgrounds and the relatively poor mass resolution, the search is preferentially conducted using final states that contain isolated leptons and photons, despite the smaller branching ratios (Fig. 1.2), and in the detection of these particular final states CMS has been optimized. In fact in each second are expected at low luminosity ($10^{33} \text{ cm}^2\text{s}^{-1}$) the production of one $t\bar{t}$ -pair, five Z bosons, which decay into lepton pairs, 50 W bosons, 100 QCD jets with a transverse momentum larger than 200 GeV and half a million $b\bar{b}$ -pairs within the CMS detector. These large rates of physics processes provide not only a good opportunity for high precision tests of the Standard Model, but are also a huge background to many hypothetical new physics channels, as discussed in [9].

However the high luminosity and the large center of mass energy of the LHC proton-proton collisions allow also the test of various theoretical models, like Supersymmetry (SUSY), that foresee the existence of an entire new class of undiscovered particles. According to this theory, particles are said to have superpartners (sparticles). Since they have not been observed so far, SUSY must be a broken symmetry, which means that sparticles have masses different than their counterparts. The SUSY masses are expected in the TeV range, which makes them visible to LHC. Theory predicts at least five SUSY Higgs bosons and it can provide an explanation for the dark matter of the universe. When colliding lead ions instead of protons, the energy density is much higher. Thus, it is expected to rebuild a very early stage of the universe called quark-gluon plasma, which may reveal different physical properties.

Another motivation is the Charge-Parity (CP) Violation. First reported in the 1960s, several experiments have measured the CP violation even if, until now, it is only possible to observe a very small effect in the decay rates of Kaon particles. LHC will enter a new energy range and serve as a huge B-factory, reaching cross section for $b\bar{b}$ pair production of the order of hundred microbarns. The LHCb experiment will be dedicated to this study.

1.3 The CMS detector

The Compact Muon Solenoid (CMS)[4] is a general-purpose detector, designed to observe all possible decay products of the LHC subatomic particles interactions (heavy ions

or protons), by covering as large an area around the interaction point as possible. It is able to detect as many particle types as possible: leptons, photons, jets, and b-quarks and isolate at each bunch crossing the events of interest for physics studies. It has been designed to be “hermetic” and provide a very good muon system whilst keeping the detector dimensions compact. The CMS structure follows the typical design used in the general purpose experiment with collider: several cylindrical layers, coaxial to the beam direction, referred as barrel layers, closed at both ends by detector disks orthogonal to the beam pipe to ensure the detector hermeticity, as shown in Fig. 1.3.

The entire detector has a full length of 21.6 m, a diameter of 14.6 m and reach a total weight of 12,500 t. Considering this particular geometry, a pseudo-angular coordinates reference frame is adopted, required by the invariant description of the pp physics. It has the origin centered at the nominal collision point inside the experiment, the y-axis pointing vertically upward, and the x-axis pointing radially inward toward the center of the LHC. Thus, the z-axis points along the beam direction toward the Jura mountains from LHC Point 5. The azimuthal angle (ϕ) is measured from the x-axis in the x-y plane. The polar angle (θ) is measured from the z-axis. Pseudorapidity is defined as $\eta = -\ln \tan(\theta/2)$. Thus, the momentum and energy measured transverse to the beam direction, denoted by p_T and E_T , respectively, are computed from the x and y components.

The detector structure is formed by the several subsystems located between the beam pipe and the solenoid magnet frame (the central tracker, the electromagnetic calorimeters (ECAL), the hadronic calorimeter (HCAL)), whereas the muon system is all around embedded in the iron yoke. Common for all multipurpose detectors is the working principle illustrated in the Fig. 1.4. Photon and electron energies are measured by the electromagnetic calorimeter, whereas the hadronic energy is mainly obtained by the hadron calorimeter. Muons are identified by chambers in the outermost detector layers. Their momenta, as well as those of other charged particles, are measured in the tracker, placed inside the magnetic field. Hence the construction is divided into several sub-detectors, each of them responsible for detection of specific particles. One of the key point of the CMS detector is the choice of the magnetic field configuration for the measurement of the momentum of muons. Large bending power is needed to measure precisely the momentum of charged particles, imposing the choice of superconducting technology for the magnets. In order to achieve good momentum resolution within a compact spectrometer without making stringent demands on muon-chamber resolution and alignment, a high magnetic field was chosen. The return field is large enough to saturate 1.5 m of iron, allowing 4 muon “stations” to be integrated to ensure robustness and full geometric coverage. Each muon station consists of several layers of aluminium drift tubes (DT) in the

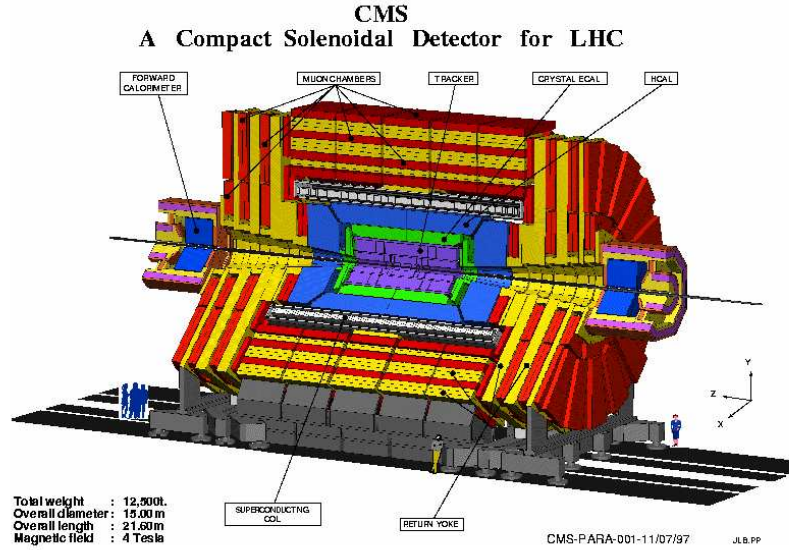


Figure 1.3. Schematic view of the CMS Detector. Close to the interaction point is an all silicon Tracker, that is surrounded by the Electromagnetic Calorimeter (ECAL) and the Hadronic Calorimeter (HCAL). All these systems are contained inside the superconducting solenoid. The detectors of the muon system: Drift Tubes (DT), Resistive Plate Chambers (RPC) and Cathode Strip Chambers (CSC) are embedded in the iron return yoke of the solenoid [4].

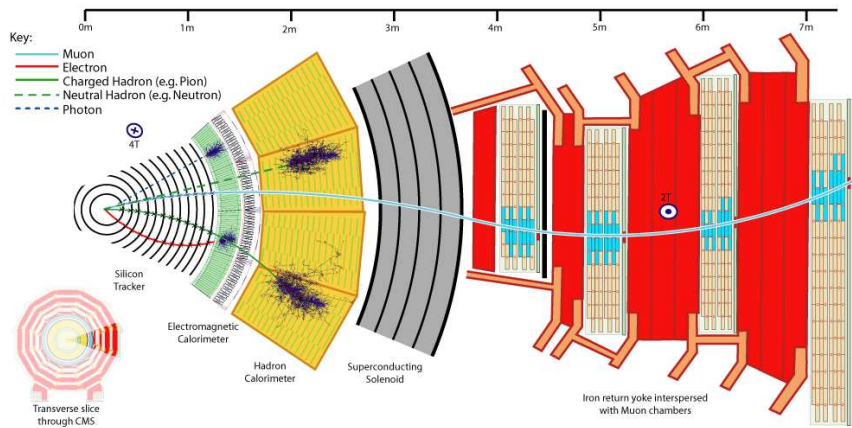


Figure 1.4. Transversal view of the CMS Detector [4].

barrel region and cathode strip chambers (CSCs) in the endcap region, complemented by resistive plate chambers (RPCs).

1.3.1 Requirements

The main distinguishing features of CMS are a high-field solenoid, a full silicon-based inner tracking system, and a fully active scintillating crystals-based electromagnetic calorimeter. These features allow to fulfill the following requirements to meet the LHC physics programme:

- Good muon identification and momentum resolution over a wide range of momenta in the region $|\eta| < 2.5$, good dimuon mass resolution (≈ 1 at $100 \text{ GeV}/c^2$), and the ability to determine unambiguously the charge of muons with $p < 1 \text{ TeV}/c$.
- Good charged particle momentum resolution and reconstruction efficiency in the inner tracker. Efficient triggering and offline tagging of τ 's and b-jets, requiring pixel detectors close to the interaction region.
- Good electromagnetic energy resolution, good diphoton and dielectron mass resolution ($\approx 1\%$ at $100 \text{ GeV}/c^2$), wide geometric coverage ($|\eta| < 2.5$), measurement of the direction of photons and/or correct localization of the primary interaction vertex, π^0 rejection and efficient photon and lepton isolation at high luminosities.
- Good E_{miss}^T and dijet mass resolution, requiring hadron calorimeters with a large hermetic geometric coverage ($|\eta| < 5$) and with fine lateral segmentation ($|\Delta\eta| \times |\Delta\phi| < 0.1 \times 0.1$).

In the next sections an overview of all CMS subdetectors from inside to outside will be given, underling the main features and peculiarity of the technology design to fulfill the LHC physic programme.

1.3.2 The Tracking system

The CMS Tracker detector [10] [11], encompassing the beam-pipe, is the closest detector to the interaction point, able to measure the trajectories and momenta of charged particles

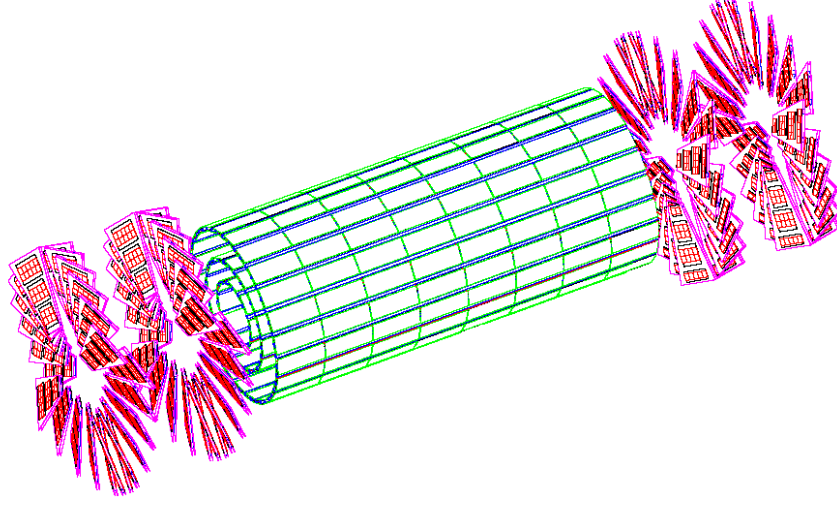


Figure 1.5. A schematic of the pixel tracker. The barrel is colored green, the endcaps red [10].

up to $|\eta| \simeq 2.4$. Its main purpose is to detect, identify and characterize the tracks and vertexes of the particles produced in the interaction. Hence it has to assure an efficient track reconstruction, needed to identify W and Z bosons, which are involved in many new physics signatures at the LHC, and a good track isolation, required to suppress the jet backgrounds to isolated high energy photons and electrons. The Tracker is composed by several silicon pixel layers close to the interaction point, surrounded by a large silicon tracking detector. Fine granularity pixels are placed closest to the interaction point, where the particle flux is highest, to maintain a low channel occupancy and minimize track ambiguities. The pixel system consists of 3 barrel layers: 4.4 cm, 7.3 cm, and 10.2 cm from the beam-pipe with a length of 53 cm and 2 endcap discs extending from 6 cm to 15 cm in radius, at $|z| = 34$ cm and 46.5 cm. Here 66 million pixels of size $\sim 100 \times 150 \mu\text{m}^2$ are arranged across 768 and 672 modules in the barrel and endcaps, respectively. To maximize vertex resolution, an almost square pixel shape has been adopted. A Lorentz angle of 23° in the barrel improves the r - ϕ resolution through charge sharing. The endcap discs are assembled with a turbine-like geometry with blades rotated by 20° to also benefit from the Lorentz effect. The resultant spatial resolution is $10 \mu\text{m}$ in r - ϕ and $20 \mu\text{m}$ in z , allowing a primary vertex resolution of $40 \mu\text{m}$ in z . The layout is illustrated in Fig. 1.5. The silicon strip tracker (SST) is divided into four main subsystems (Fig. 1.6). The central region is made of the Inner Barrel (TIB), that extends from $r=20\text{cm}$ to $r=55\text{cm}$ and is composed of four layers, and the Outer Barrel (TOB), that extends to $r=116\text{cm}$ and consists of six layers. In the forward region, the Inner Disks (TID) and the Endcaps (TEC)

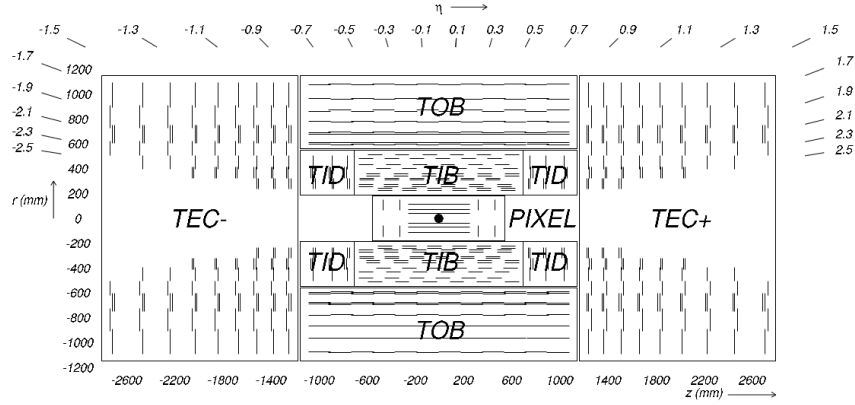


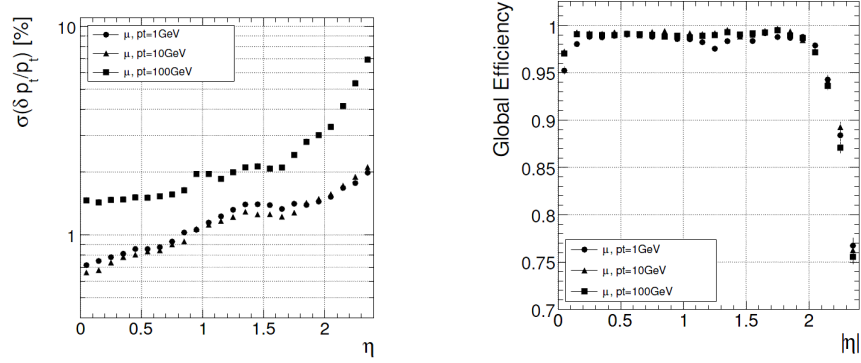
Figure 1.6. Schematic cross-section through the CMS tracker. Each line represents a detector module [10].

are made of respectively three and seven disks, up to $|z|=282\text{cm}$. There are 24244 single-sided micro-strip sensors covering an active area of 198m^2 . Throughout the tracker, the strip pitch varies from the inner to the outer layers (from $80\mu\text{m}$ to $205\mu\text{m}$) in order to cope with the anticipated occupancy and to grant a good two-hit resolution. The size of the device has led to a design where the basic unit, called a module, houses the silicon sensors and the readout electronics, for a total of 15148 modules.

Representative results of the tracker performances are illustrated in Fig. 1.7a, which shows the transverse momentum in the $r\text{-}\phi$ and z planes for single muons with a p_T up to $100\text{ GeV}/c$, as a function of pseudorapidity. Track reconstruction efficiency as a function of pseudorapidity for single muons is shown in Fig. 1.7b.

1.3.3 The Calorimeters

Inside the solenoid magnet of about 6 m diameter, two calorimeters measure the energy of particles produced in the interaction.



(a) Resolution of several track parameters for single muons with transverse momenta of 1, 10 and 100 GeV/c [10].

(b) Global track reconstruction efficiency for muons of transverse momenta of 1, 10 and 100 GeV/c [10].

Figure 1.7. Tracker performance [11].

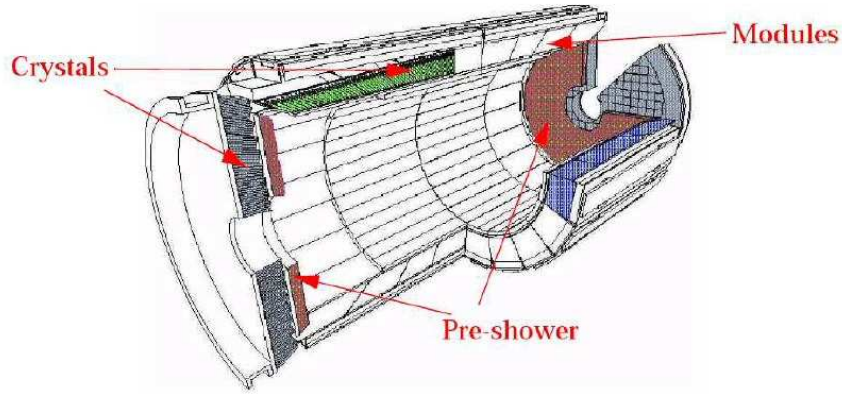


Figure 1.8. The CMS electromagnetic calorimeter [4].

ECAL

The CMS Electromagnetic Calorimeter [12] is designed to provide very precise energy measurement of electrons and photons. It will consist of about 76000 Lead Tungstate (PbWO₄) crystals with pointing geometry, arranged in a Barrel part and two Endcaps (Fig. 1.8). The design can be kept compact, since PbWO₄ is a dense material ($\rho = 8.3 \text{ g cm}^{-3}$). The crystals have a short radiation length ($X_0 = 8.9 \text{ mm}$) and Moliere radius (RM = 2.19 mm), which allows the construction of a compact and highly granular detector. The scintillation light decay time is approximately 10 ns, the peak emission is at 440 nm while 80% of the light is emitted in 25 ns. The crystals have a light yield (LY) of $9.3 \pm 0.8 \text{ pe/MeV}$ so photo-detectors with intrinsic gain are required. The scintillation light is collected by Silicon Avalanche Photo-Diodes (APDs) in the Barrel and Vacuum Photo-Triodes (VPTs) in the Endcaps. Especially for low Higgs masses $m_{H^0} \leq 150 \text{ GeV}$, the decay channel $H^0 \rightarrow \gamma\gamma$ plays an important role due to its clear signature. Its identification requires good energy resolution, which is provided by the ECAL and can be described by

$$\frac{\sigma}{E} = \frac{S}{\sqrt{E}} \oplus \frac{N}{E} \oplus C$$

with a stochastic term S, noise N and constant term C. The target performance for the energy resolution is a stochastic term of 2.7% (5.7%), a noise term of 155 (770) MeV and a constant term of 0.55% (0.55%) for the ECAL Barrel (Endcap). Representative results on the energy resolution as a function of the beam energy are shown in Fig. 1.10a.

HCAL

The Hadronic Calorimeter (HCAL)[13] plays an essential role in the identification and the measurement of quark, gluons, and neutrinos by measuring the energy and the direction of jets and of missing transverse energy flow in events. The showers of strongly interacting particles, like pions, kaons, protons or neutrons, are contained inside the hadronic calorimeter HCAL. The hadron calorimeter barrel and endcaps sit behind the tracker and the electromagnetic calorimeter as seen from the interaction point. The hadron calorimeter barrel is radially restricted between the outer extent of the electromagnetic calorimeter ($R = 1.77 \text{ m}$) and the inner extent of the magnet coil ($R = 2.95 \text{ m}$). This constrains the total amount of material which can be put in to absorb the hadronic shower. Therefore, an outer hadron calorimeter or tail catcher is placed outside the solenoid complementing the barrel calorimeter. To provide good hermeticity, very forward calorimeters are placed

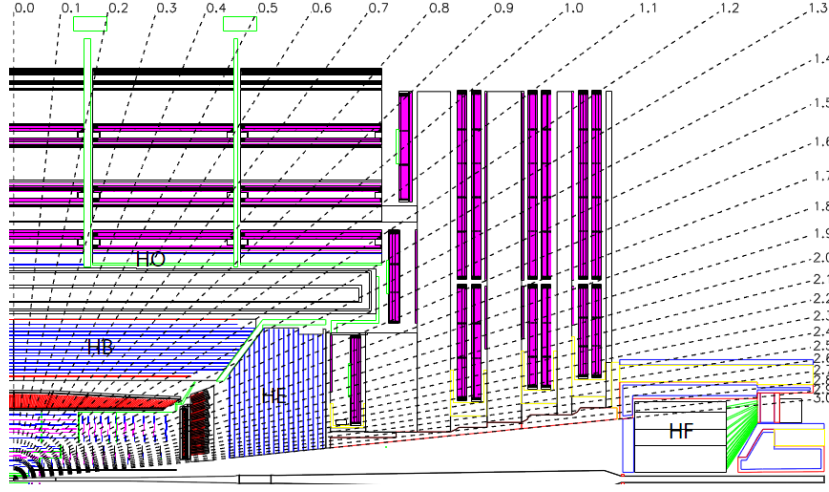


Figure 1.9. Longitudinal view of the CMS detector showing the locations of the hadron barrel (HB), endcap (HE), outer (HO) and forward (HF) calorimeters [12].

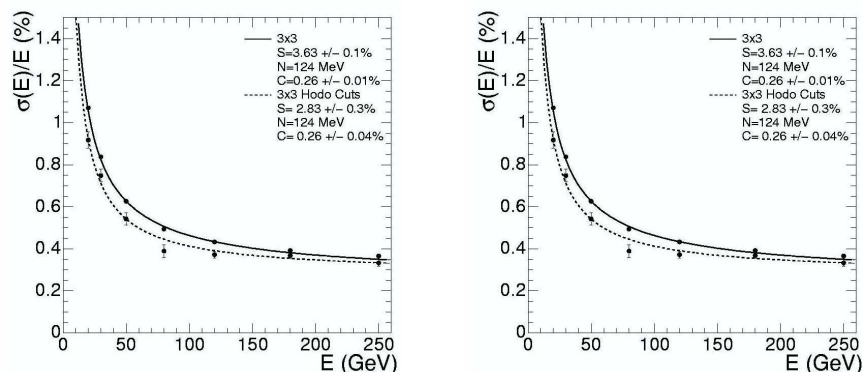
close to the beam pipe, covering the range from $3.0 \leq |\eta| \leq 5.0$, as shown in Fig. 1.9. In the HCAL, brass absorber plates are interleaved with 3.7 mm thin plastic scintillators tiles, which are read out by wavelength-shifting fibres (WLS) in the barrel and endcap region. In the forward calorimeter quartz fibres are embedded in a steel absorber matrix and the emitted Cerenkov light is guided by fibres to photomultipliers. The performances of the HCAL is shown in diagram 1.10b, where the jet transverse energy resolution is plotted versus the simulated transverse energy for different detector regions. The curves show the typical $1/\sqrt{E}$ behavior and for high particle energies, $E_T \geq 50$ GeV, 10 - 20 % resolution can be achieved, depending on the detector region. The hadronic energy resolution combined with ECAL measurements [4] is

$$\frac{\sigma}{E} = \frac{100\%}{\sqrt{E[\text{GeV}]}} \oplus 4.5\%$$

and it is expected to sensibly degrade around $|\eta| = 1.4$, where there will be installed services and cables resulting in a higher amount of inactive material. The performance of the very forward calorimeter

$$\frac{\sigma}{E} = \frac{182\%}{\sqrt{E[\text{GeV}]}} \oplus 9\%(\text{hadrons}) \quad \frac{\sigma}{E} = \frac{138\%}{\sqrt{E[\text{GeV}]}} \oplus 5\%(\text{electrons})$$

is sufficient to improve the missing transverse energy resolution to the desired level.



(a) ECAL supermodule energy resolution, σ_E/E , as a function of the electron energy as measured from a beam test (b) HCAL resolution as function of particle energy in different detector regions for simulated jet.

Figure 1.10. Calorimeter resolutions [13].

1.3.4 The Magnet

The CMS magnet [14] is a large superconducting solenoid with a diameter of 5.9 m. It provides an inner uniform 4 T magnetic field obtained with a current of 20 kA. The main features of the CMS solenoid are a central flat superconducting cable, an high purity aluminium stabilizer and an external aluminium-alloy to reinforce the sheath. The superconducting cable is a Rutherford type with 40 NiTb strands and is kept cooled by a liquid helium cryogenic system. The magnetic flux is closed in a loop via a 1.8 m thick saturated iron yoke, instrumented with four muon stations. The bore of the magnet coil is also large enough to accommodate the inner tracker and the calorimetry inside.

1.3.5 The Muon System

One of the most strictly requirements for CMS [15] is to have a robust muon system since muons represent a cleanest signature of many physics channels such as the Higgs decay to two vector bosons ($H \rightarrow ZZ \rightarrow 4l$, $H \rightarrow WW$) and are a reliable observable for triggering purposes. In order to achieve good physics performances, a standalone resolution of

9% at 200 GeV and from 15 to 40% at 1 TeV in the measurement of the muon transverse momentum is required. Global resolutions of 1% at low p_T and around 5% at 1 TeV would hence be obtained in combined measurement with the tracker. The muon trigger must have no dead time in order to cope with the 40 MHz collision rate. Muon identification and charge assignment must be granted up to 7 TeV in $|\eta| < 2.4$. A very hermetic and redundant detector is therefore mandatory. On top of that, the detectors must work in hostile environments, with magnetic field up to 3.5T and muon rate up to 1000 Hz/cm² in the endcaps. The constraints are less severe in the barrel, where the magnetic field is much lower and the expected muon rate will not be above 1 Hz/cm². In CMS three different types of detector technologies were chosen to this purpose (Fig. 1.11) and to build a redundant system: for the tracking and triggering of muons, Drift Tube chambers (DT) in the barrel region ($|\eta| < 1.2$) and Cathode Strip Chambers (CSC) in the forward endcaps ($0.9 < |\eta| < 2.4$) form the muon spectrometer. Additionally, both in the barrel and endcap regions, Resistive Plate Chambers (RPC) are installed with the aim of complementing the muon detector with a fast trigger-dedicated detector. The single muons identification efficiency in the muon system as a function of the muon pseudorapidity is showed in Fig. 1.12a whereas in Fig. 1.12b the transverse momentum resolution of the muon tracks as function of increasing p_t is presented with and without tracker information. In Fig. 1.12a the muons were generated flat in the intervals $5 < p_T < 100$ GeV/c and $|\eta| < 2.4$, and the average identification efficiency of the Global Muon Trigger is 98.3%; the losses of efficiency in some $|\eta|$ regions are due to the gaps between the muon chambers.

Drift Tube

The DT chambers are inserted in the pockets of the 5 slices (“wheels”) that form the magnet return yoke. They are distributed in 4 concentric layers (“stations”) with respect to the beam line, segmented in 12 sectors. It makes a total of 250 chambers. High p_T muons will cross up to four stations in the barrel region. DTs are composed of rectangular drift cells with a maximum drift time of 380 ns. The cells are distributed in 4 staggered layers, forming independent measurement units called “Super-Layers” (SL). Each DT chamber is composed of three of these SL, two of them with their sense wires oriented in parallel to the beam line, measuring the track projection in the r - ϕ plane, and another one with wires placed in the transverse direction, measuring the coordinate in the r - ϕ plane. Superlayers are glued together with a honeycomb panel ensuring planarity and rigidity. A local track is formed by the intersection of the different points measured in each layer. Up to 12 points per muon track in each station provide the necessary redundancy. The

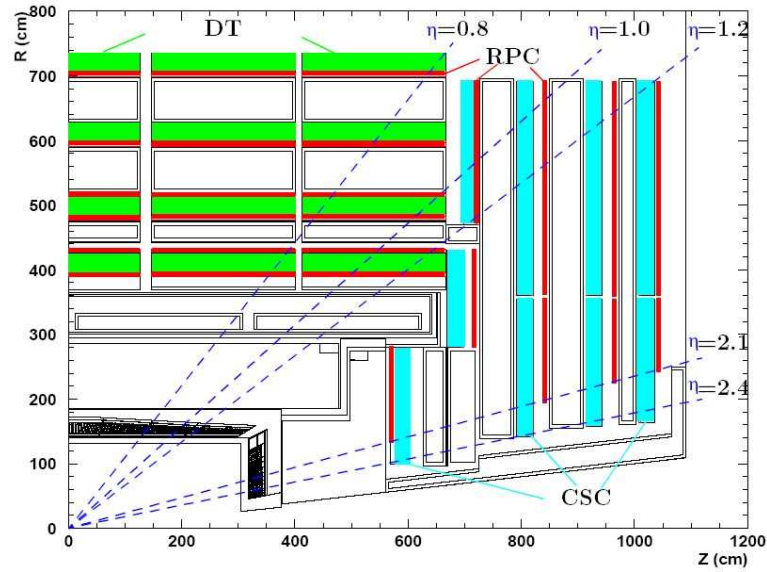
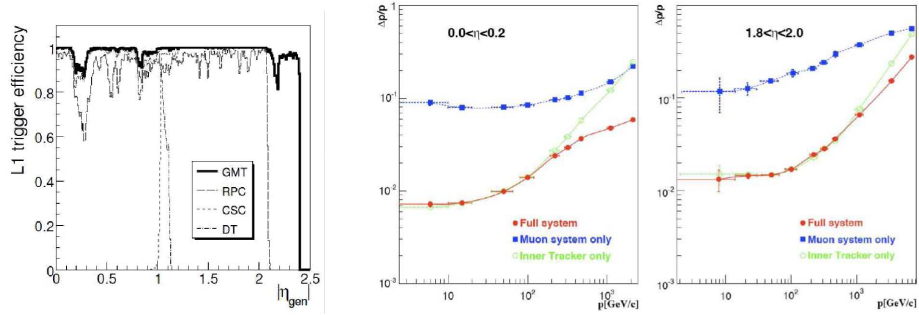


Figure 1.11. Longitudinal view of a quarter of the muon system, subdivided into barrel, with drift tubes (DT) and resistive plate chambers (RPC), and endcap with cathode strip chambers (CSC) and RPCs [15].

different trigger candidates in each chamber are selected and propagated with no dead time to subsequent levels. The final selection of the DT muon trigger propagates the best 4 muon candidates per bunch crossing to the global muon trigger.

Resistive Plate Chambers

The system is completed by Resistive Plate Chambers (RPCs) both in barrel and endcap zones, granting redundancy and fast performance in the trigger system. In the barrel region RPCs and DTs are coupled together, having each DT one or two RPC planes. In the endcaps, similarly to CSCs, RPCs are installed on the faces of the iron disks. A maximum of 6 RPC planes in the barrel and 3 planes in the endcaps are crossed by high momentum muons. In total, 480 chambers in the barrel and 432 in the endcaps constitute the whole system. The RPCs work in avalanche mode in order to cope with high background rates, while ensuring excellent time resolution (better than 1.5 ns), and precise bunch crossing assignment. A space resolution of the order of 1 cm is adequate for triggering purposes. An exhaustive description of the system, performances and the design issues will be presented in the next chapters.



(a) Efficiency for identifying single muons as a function of the muon pseudorapidity for the Global Muon Trigger (solid line) and for the DT, CSC, and RPC trigger subsystems.

(b) The transverse momentum resolution of the muon tracks.

Figure 1.12. Muon System Performances [15].

Cathode Strip Chambers

Cathode Strip Chambers CSCs are installed on the endcap disks of CMS. They are distributed in concentric rings of 18 or 36 chambers, 3 rings in the internal face (ME1), 2 more in the middle disks (ME2, ME3) and one more ring in the far high eta region (ME4), covering from 0.9 to 2.4 in pseudorapidity. Except for the outermost ring in ME1, chambers in the same ring have a certain overlap region, leaving almost no dead zones. There is a total of 468 chambers. Each CSC is a multiwire proportional chamber with trapezoidal shape, composed of 6 gas gaps, each one equipped with a layer of cathode strips running in radial direction. The strip width varies from 3.2mm to 16mm in the furthestmost points. Also for each gas gap there are anode wires of variable length running in perpendicular to the strips (except in the innermost station ME1/1, where they are tilted by 25 degrees in order to compensate for the Lorentz effect). The wire separation can be 2.5 or 3.175 mm, depending on chamber type. Each crossing muon can provide up to 6 spatial points per chamber. The point is obtained combining the cathode strips and anode wire signals. The cathode strips collect the charge induced in the gas by the crossing muon, and by charge interpolation in three-strip clusters a very precise measurement (between 80 and 450 microns) is obtained. The anode coordinate is provided by the combined readout of wire groups (from 5 to 17 wires). The wire measurement is less precise, but faster. A spatial resolution of about $100 \mu\text{m}$ per chamber is obtained. Similarly to DTs, CSC work not only as muon trackers but also as trigger detectors, assuring the redundancy to the muon system.

1.4 The CMS Online Trigger and Data Acquisition (TriDAS)

The CMS Trigger and Data Acquisition (TriDAQ) [16] system is designed to collect and analyze the detector information at the LHC bunch crossing frequency of 40 MHz. The small rate of the interesting events and the actual limitation in the storage and processing of the resulting data, require an online selection for a large fraction of them. This task is quite difficult not only due to the high rejection factors it requires (10^7), but also because the output rate is almost saturated already by standard processes like Z and W production. Therefore the trigger, in order to make its decision, should have a level of sophistication comparable to offline reconstruction, even if the time available to perform this selection is limited. The accept/reject decision will be taken in several steps (levels) of increasing refinement, where each one takes a decision using only a subsample of the available data. Another crucial function of the DAQ system is the operation of a Detector Control System (DCS) for the supervision of all detector components and the general infrastructure of the experiment. The DCS is a key element for the operation of CMS, and guarantees its safe operation and that high-quality physics data are obtained. CMS has decided to split the full selection task in two steps: Level-1 Trigger and High Level Trigger (HLT) as shown in Fig. 1.13a.

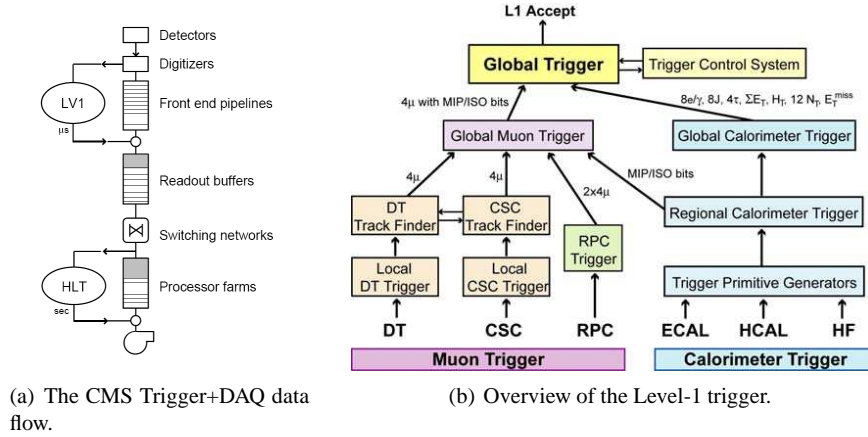


Figure 1.13. The CMS Trigger system [16].

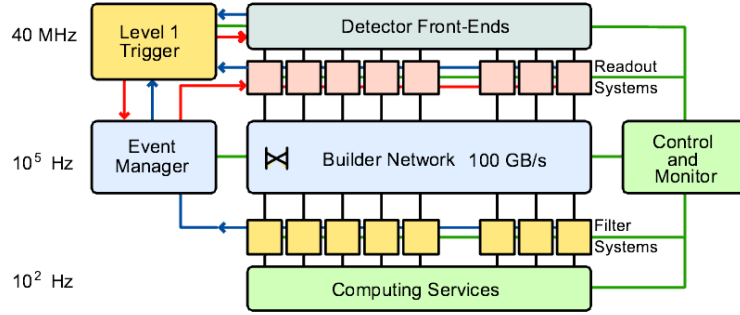


Figure 1.14. Data flow in the CMS Trigger/DAQ system. The software-based High-Level Trigger (HLT) filters via the Data Acquisition system (DAQ) the events passing hardware based Level-1 trigger [16].

1.4.1 The Level 1 Trigger

The Level-1 trigger [17] is implemented on custom-built programmable hardware. It runs dead-time free and has to take an accept/reject decision for each bunch crossing, i.e. every 25 ns. At every bunch crossing, each processing element passes its results to the next element and receives a new event to analyze. During this process, the complete detector data are stored in pipeline memories, whose depth is technically limited to 128 bunch crossings. The Level-1 decision is therefore taken after a fixed time of $3.2 \mu\text{s}$. This time must include also the transmission time between the detector and the counting room (a cable path of up to 90 m each way) and, in the case of Drift Tube detectors, the electron drift times (up to 400 ns). The time available for calculations can therefore be as low as $1 \mu\text{s}$. The Level-1 trigger is divided into three subsystems: the Calorimeter Trigger, the Muon Trigger and the Global Trigger (Fig. 1.13b). The Calorimeter and Muon Triggers identify trigger objects of different types: isolated and nonisolated electrons/photons, jets, and muons. The four best candidates of each type are selected and sent to the Global Trigger, 42 together with the measurement of their position, transverse energy or momentum and a quality word. The Global Trigger also receives the total and missing transverse energy measurement from the Calorimeter Trigger. The Global Trigger selects the events according to programmable trigger conditions, that can include requirements on the presence of several different objects with energies or momenta above predefined thresholds. In total 128 algorithm will be provided, each representing a complete physics trigger condition and a final logical OR is applied to them to generate the L1 accept signal.

1.4.2 The High Level Trigger

The second trigger level, the High Level Trigger (HLT), provides further rate reduction by analyzing full granularity detector data by means of software reconstruction and filtering algorithms running on a large computing cluster consisting of commercial processors, the Event Filter Farm. In fact once the acceptance signal is generated by the L1 trigger, the data from the front-end electronics are readout to the HLT filter farm, as shown in Fig. 1.14. It aims to execute online physics selection algorithms on the events read out, in order to accept the ones with the most interesting physics content and discard as soon as possible the other events. It is done reconstructing, whenever it is possible, only those objects and regions of the detector that are actually needed to be reconstructed. This leads to the idea of partial reconstruction and to the notion of many virtual trigger levels, e.g., calorimeter and muon information are used, followed by use of the tracker pixel data and finally the use of the full event information (including full tracking). The full detector data, (1MB) corresponding to the events accepted by the L1T, read out by the DAQ system at a rate up to 100 kHz, are at this stage output at 100Hz, sustainable by the actual mass storage devices. Events accepted by the HLT are forwarded to the Storage Managers (SM), which stream event data on disk and eventually transfer raw data files to the CMS Tier-0 computing center at CERN for permanent storage and offline processing.

Chapter 2

THE CMS EXPERIMENT CONTROL SYSTEM

The CMS Experiment Control System (ECS) is a complex distributed control system in charge for the configuration and monitoring of all the sub-detectors and equipments involved in the experiment operation, like Trigger, DAQ system, and the auxiliary infrastructures. The use of a common online framework, able to handle the entire operations in the online activities, is a fundamental requirement in a such huge system where all these activities have to be synchronized among them and with the detectors operations. Moreover, all the components are designed in a way such that its hardware implementation can be staged as the LHC accelerator luminosity increases as well as the experiment's need for higher throughput and the future technologies evolution. Hence it must be highly scalable and also support diverse hardware bases. Integrated in the DAQ computers network, it is composed by the Run Control and Monitor System (RCMS), the Detector Control System (DCS), a distributed processing environment (XDAQ), and the sub-system On-line Software Infrastructure (OSWI), as illustrated in Fig. 2.1 . These components and their integration in the CMS DAQ are described in the following sections.

2.1 Data Acquisition System (DAQ)

The DAQ system is the first place where the entire information from the physics collisions can be inspected and monitored, thus providing early feedback to physicists running the

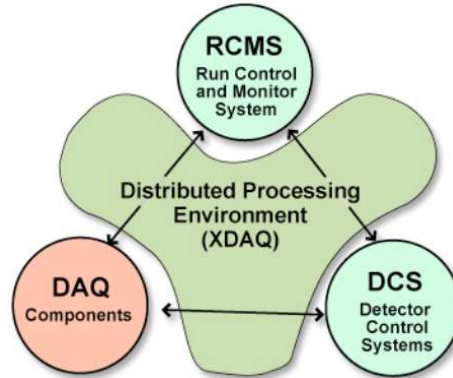


Figure 2.1. Overall online software architecture. Circles represent sub-systems that are connected via XDAQ [16].

experiment. The DAQ is in fact the first system of CMS that implements the two crucial functions, that eventually determine the reach of the physics program: event selection, and control and monitoring of the CMS detector elements, as described in Fig. 2.3. The design of the DAQ must therefore address widely different requirements, varying from the fast transfer of large amounts of data, to provide resources for the intelligent filtering of this data, record the selected data and finally present an intuitive, functional and powerful interface to physicists running the data taking.

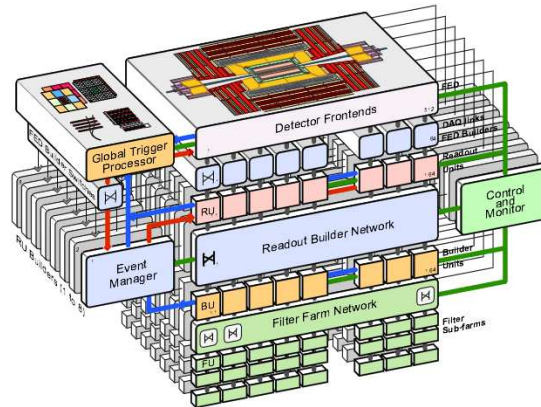


Figure 2.2. DAQ scheme highlighting the “slices” structure [16].

Its architecture is composed by different building blocks, with different aims, where the

data are transmitted and processed. First stage corresponds to the readout of the data from the sub-detectors front-end systems. Once the synchronous L1 trigger acceptance signal is generated via the Timing, Trigger and Control (TTC) system [18], the data are extracted from the front-end buffers and pushed into the DAQ system by the Front-End Drivers (FEDs). At each trigger, the whole CMS detectors' information for a given bunch crossing, containing the digitalized data of the signal collected and the relative delay due to the trigger offset and time of flight delay, is read out. All the data of a single event, spread over ≈ 700 FEDs, are sent to the Builder unit. The event builder assembles the event fragments belonging to the same L1 from all FEDs into a complete event and transmits it to one Filter Unit (FU) in the Event Filter for further processing. Once a Filter Unit receives an event, it performs the High Level Trigger algorithms and decides whether to trash it or to forward it to the Computing Services. Also an unbiased random sample of events are forwarded regardless of the HLT. This is used for the twofold purpose of checking the quality of HLT algorithms and monitor the detector. All the events which passed the Filter System are stored and a fraction of them is analyzed online in order to monitor the quality of collected data. The Computing Services also perform the calibration and alignment of the detectors. Both these operations are crucial in order to push the detector performances to the design requirements. There are two additional systems following the data flow from the front end to the Computing Services: these are the Event Manager, which monitors the data flow through the DAQ and the Control and Monitor, which is devoted to the configuration and monitoring of all the elements and will be described in the next section.

2.1.1 Cross-platform DAQ framework

The complexity of the DAQ system and the different sub-system with whom it has to communicate, require a common and ad-hoc software environment to facilitate the efficient control of CMS and the data taking operation. For this purposes, CMS has developed an in-house domain-specific middleware, XDAQ (Cross-Platform DAQ Framework) [19], able to match the different requirements of the data acquisition applications and to provide to all CMS subsystems a common environment where to develop the custom applications. It is used by the different sub-systems for communication, configuration, control, and monitoring. The central DAQ and each sub-system local DAQ are developed in XDAQ as well as the sub-detector electronics configuration and monitoring components (FEC and FED), and the trigger supervisor architecture. Written entirely in C++, it provides applications with efficient, asynchronous communication in a platform independent way, thanks

to the use of the SOAP/http [20] protocol and Intelligent Input/Output (I_2O) protocol [21] over TCP/IP, widely used in Web applications. A rich set of data structures, including lists, vectors and histograms are exportable and can be inspected by clients through the executive SOAP services. Additional utility components provide support for hardware and database access, allowing the developer to focus on providing an application layer that exposes the hardware functionalities. In addition to this, XDAQ also provides a web interface, HyperDAQ, and a generic Finite State Machine (FSM) functionality, allowing the CMS detector and DAQ to be globally configured, enabled and disabled from a single point of control.

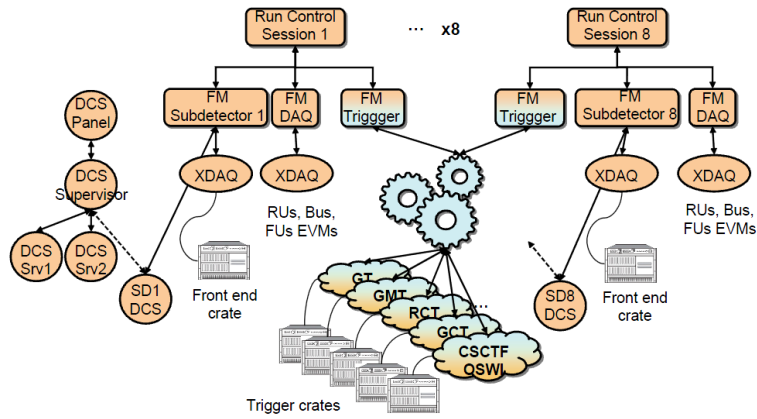


Figure 2.3. Architecture of the CMS Experiment Control System [19].

2.2 Run Control and Monitoring System

The Run Control and Monitor System (RCMS) [22] is the collection of hardware and software components responsible for controlling and monitoring the CMS experiment during data taking. It allows to operate the experiment and to monitor the detector and data taking status through a single interface. The main requirements are:

- Provide interactive graphical user interfaces to operate the entire CMS experiment,
- Manage the correct configuration of all components and synchronize all the operations,

Figure 2.4. Typical GUI for data taking operation control [22].

2.2.1 Architecture and Functionalities

Because of the complexity and the huge number of applications under its control ($O(10^4)$ applications, running on $O(10^3)$ PCs), the RCMS is organized into several different sub-systems: a sub-system can be corresponding to a subdetectors, e.g. to the Hadron Calorime-

ter, or to a partition like central DAQ or global trigger. Its structure is implemented as a tree of finite state machines by means of RCMS controls the data taking operation of the experiment, as shown in Fig. 2.5. All the operation are handled by a “Function Manager” (FM), characterized by finite state machine and a set of services. Each FM is in charge, during the data taking, to prepare the respective subsystem with the right configuration and synchronize it with all the other sub-systems under the RCMS control. The hierarchical structure indeed assures scalability of the system, thus it can be easily expanded by adding additional components. Different functionalities are available from each FM in order to accomplish the standard control operation: access control, configuration, monitoring, error handling, logging and synchronization with other subsystems. All of these are configurable by the sub-system experts even if a standardized state machine model has been adopted by the sub-system for the first level of FMs, in order to assure communication and homogeneity between different levels. One of the main tasks of the RCMS is the start and configuration operations of all the online processes of the DAQ and the sub-detectors during the data taking operation. It is provided via a key mechanism, based on the loading of predefined configuration for each subsystem, that allows the partitionability of the system and an easy handling of the operations. In this way in fact specific configurations can be prepared for the different subsystem according to the different data taking scenarios and physics performances to be accomplished.

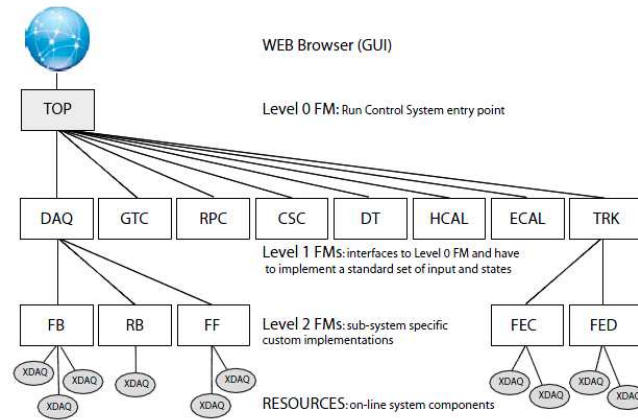


Figure 2.5. The RC hierarchy showing the full DAQ system. The Top Function Manager controls the next layer (Level 1) of Function Managers who in turn control the Level 2 (sub-detector level) Function Managers. The sub-detector Function Managers are responsible for managing the online system component resources. [22]

2.2.2 Software Components

Because of the complexity and of the different functionalities provided by the RCMS, the software architecture is developed using different technologies and programming environments. The Run Control applications and services are implemented in Java as components of a common web application “RCMS” provided by the framework. Web technologies and related developments play a strong role in the implementation of the RCMS and tools and solutions based on Web technologies are largely used in the framework. The interface is indeed based on the Web Service Description Language (WSDL) using the Apache Axis [24] implementation of Web Services (WS) and the Java Servlet technology Tomcat [25] as platform, allowing different web clients, developed in different programming languages or frameworks like Java, LabView and Perl, to access to the Run Control services. The storage of the key and the loading of the configurations are instead developed using both MySQL and Oracle technologies to assure persistency of the data and the correctness and reliability for the thousands of parameters handled. One common database (Oracle) is shared by all online processes and RCMS installations.

2.3 Detector Control System

The Detector Control System (DCS) [26] is aimed to provide a complete control over all subdetectors, all infrastructure and services needed for the CMS operation, its active elements, the electronics on and off the detector, the experimental hall as well as communications with the accelerator. All operator actions on the detector will be through DCS. Similarly, the presentation of all error messages, warnings and alarms to the operator will be notified by the DCS. The protection of the apparatus is the responsibility of each subsystem. Many of the functions provided by DCS are needed at all times, and as a result selected parts of the DCS must function continually on a 24-hour basis during the entire year. It is integrated in the DAQ system as an independent partition (Fig. 2.6), and during data taking, is supervised by the RCMS that instructs it to set up and monitor partitions corresponding to the detector elements needed for the data taking run.

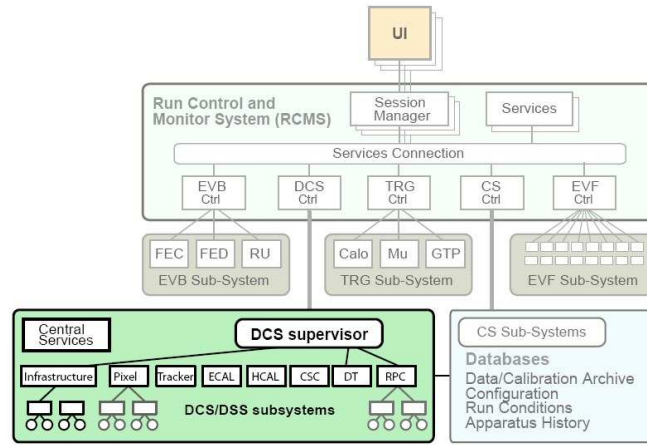


Figure 2.6. Overall online software architecture. Circles represent sub-systems that are connected via XDAQ [26].

2.3.1 Mission and Requirements

Several are the requirements imposed for such system according to the complexity and the importance of the task to accomplish. First and foremost, the DCS has to assure reliability at the experiment operation and provide safe power, redundancy and reliable hardware in numerous places. It has also to be modular and partitionable in order to allow independent control of individual subdetectors or part of them and an easy integration of new components. Another crucial point is the automatization of the procedure and action required to act on it, required to speed up the execution of commonly action and to avoid mostly human mistakes in such repetitive action. From the usability point of view, it must provide generic interfaces to the other system, e.g. the accelerator, the magnet, the RCMS, and has to be easy to operate, allowing also to the non experts to be able to control the routine operation. Finally it has to be easy to maintain and to integrate with new features, favouring the usage of commercial hardware and software components that assure reliability and easy maintenance for the components along all the CMS life time.

2.3.2 Architecture and Functionalities

The architecture of the DCS and the technologies used for its implementation are strongly constrained by environmental and functional reasons. The heart of the control operation

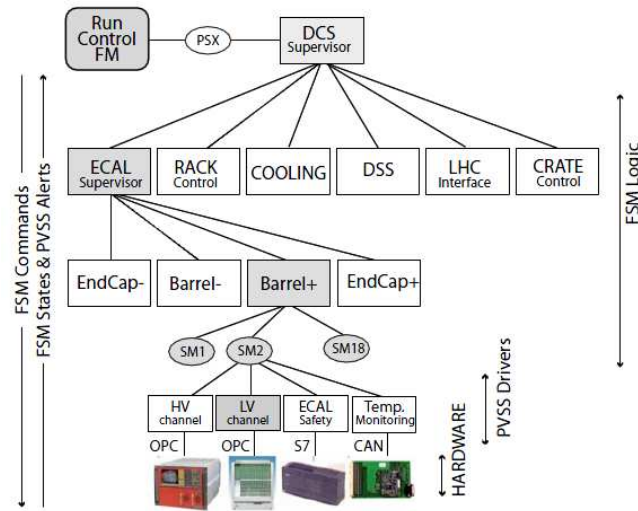


Figure 2.7. Outline of the Detector Control System hierarchy. Shown are all global services and ECAL as an example of a sub-detector control [26].

consists of a distributed Supervisory Control And Data Acquisition system (SCADA) running on PCs and called Back-End (BE), and of the Front-End (FE) systems. The name SCADA indicates that the functionality is two-fold: It acquires the data from the front-end equipment and it offers supervisory control functions, such as data processing, presenting, storing and archiving. This enables the handling of commands, messages and alarms. The detector control system architecture is developed in a hierarchical structure where at the top the Central DCS Supervisor controls the single subdetectors trees and interact with the RCMS, as described in Fig. 2.7. These sub-detector DCS subsystems control all the individual detector services and electronics, such as the power supplies, both commercial and custom made, and all the auxiliary systems required to the detector operation. Additional components such as front-end detector read-out links are also monitored by the DCS.

The detector controls are organized in a tree-like FSM node hierarchy representing the logical structure of the detector, where commands flow down and states and alarms are propagated upwards. FSM trees are created using logical FSM nodes to model the control logic plus FSM device leaf nodes connected to hardware. All the subdetectors control systems are integrated in a single control tree headed by the central DCS to ensure a homogeneous and coherent experiment operation. The DCS is in charge also of the detector configuration during the start up operation and for the data taking preparation of

many DCS front-end components and their power supplies. This is required either to bring them into a running condition or to simply define their running mode. These configurations are performed as in the RCMS by mean of predefined configurations, stored in a configuration database and loaded automatically through the FSM. Monitoring of the working condition is another crucial task performed by the DCS. The DCS instrumentation consists of a wide variety of equipment, from simple front-end elements like sensors and actuators, up to complex computer systems that are connected to the SCADA stations by means of standard fieldbuses. It provides both bookkeeping of detector parameters and safety-related and automatic functions, including alarm handling and limiting the control of critical components via a software access control. Therefore, selected data from DCS is exported to the CMS conditions database, which contains all the data describing the detector environment needed for the offline reconstruction and for studying the detector response and for tuning its physical behavior. Many of the features provided by the DCS are needed at all times, and as a result selected parts of the DCS must function continually on a 24-hour basis during the entire year. To ensure this continuity UPS and redundant software and hardware systems are implemented in critical areas, however even non-critical nodes can be recovered in the order of minutes thanks to a CMS specific automated software recovery system. In total the DCS supervises $\approx O(10^4)$ hardware channels, described by $\approx O(10^6)$ parameters, through about 100 PCs with the majority of them running Microsoft Windows, although Linux is also supported. The software architecture, used to fulfill these tasks, is described in the next paragraphs.

2.3.3 Software Framework

PVSS

PVSS is a Supervisory Control And Data Acquisition (SCADA) application designed by ETM of the Siemens group [27] and used extensively in industry for the supervision and control of industrial processes. The CERN decided to adopt for all the LHC control systems this common SCADA solution in order to provide a flexible, distributed and open architecture, easy to customize to a particular application area. PVSS is mostly used to connect to hardware (or software) devices under the DCS control, acquire the data they produce and use it for their supervision, i.e. to monitor their behaviour and to initialize, configure and operate them. PVSS has a highly distributed architecture and a PVSS application is composed of several software processes called Managers. Its software ar-

chitecture is based on a PVSS project, running on a single pc, and composed by several processes, called “Managers” with specific purposes, as described in Fig. 2.8. Different types of Managers may be used for each single project and the resources can be split over different projects in order to avoid unnecessary overhead.

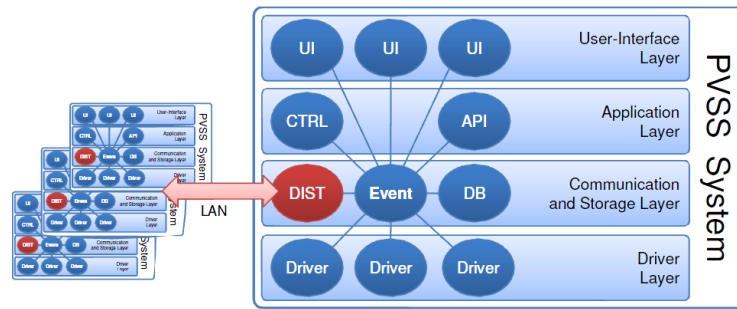


Figure 2.8. PVSS Manager structure showing the respective functional layers. Several Projects can be connected via LAN to form a Distributed System [27].

The Event Manager (EV) is the PVSS central processing unit, that handle the intercommunication among all the other managers in the same project and manage the process variables in the memory. Data flow, commands and alert condition are handled and orchestrated by the EV, as well as the broadcasting of this data towards the drivers managers. The device data in the PVSS database is structured as Data Points (DPs) of a predefined Data Point Type (DPT). PVSS allows devices to be defined using these DPTs, similar to structures in Object Oriented programming languages. It describes the data structure of the device and a DP contains the information related to a particular instance of such a device (DPs are similar to objects instantiated from structure in OO terminology). The DPT structure is user definable and can be as complex as one requires and may also be hierarchical. Data processing is performed in an event-based approach using multithreaded callback routines upon value changes, reducing the processing and communication load during the steady-state operation with no changes. The communication among the different project inside the distributed system is handled via TCP/IP protocol by a “Distribution” Manager , allowing to remotely access the data and events of all connected Projects. The persistency of the data acquired is assured by an “Data Manager” that stores data into a relational database and allows for the information to be read back into PVSS, e.g. trending plots, for the diagnostic purposes or for quality data check. In addition the possibility to connect to a relation database permits data access from other

sources for configuration and detector calibration purposes. In order to interface with the FE hardware, PVSS offers a number of Managers as “Drivers” interface for data read-out of the most used industry standard protocols like Profibus, CanBus, DIM, Modbus, for communication with Programmable Logic Controllers (PLC), and OPC are available. PVSS offers the possibility to accomplish specific tasks through an additional application layer, based on C-like scripting, called “Control”. It is based on a multithreading ANSI C-like scripting language and allows to define background scripts, able to access to the project database and all the system variables and operate on them at run-time level while at the same time protecting the low level data acquisition and processing. The usability and the human readability of the system data is accomplished through The User Interface (UI) layer. It offers, by mean of panels, widgets, synoptic diagrams and graphical objects, the possibility to define the operator interface level to display control system conditions and processes to an operator. Any UI allows the correct operation on the system by not expert and protected the hardware by mean of an access control mechanism, restricting the interaction with all other Managers according to predefined privileges. PVSS provides also a API Manager that allows the users to write their own programs in C++ and access the data in the PVSS database. On this way CMS has design the specific communication mechanism between DCS and external entities, based on the PVSS SOAP interface (PSX). The PSX is a SOAP server implemented with XDAQ using the PVSS native interface and JCOP framework, and allows access to the entire system via SOAP.

JCOP

Because of the common tasks and requirements for control among all the LHC experiment, the Joint Controls Project (JCOP)[28] was created in order to provide a set of facilities, tools and guidelines in the experiment control system development to develop an homogeneous and coherent system. The project main aims are to reduce the development effort, by reusing common components and hiding the complexity of the underlying tools, and obtain a homogeneous control system that will ease the operation and maintenance of the experiments during their life span. The JCOP enhances the PVSS functionalities providing several tools and a common framework, as illustrate in Fig. 2.9. It defines also guidelines for development, alarm handling, control access and partitioning, to facilitate the development of specific components coherently in view of its integration in the final, complete system. The framework includes PVSS components to control and monitor the most commonly used commercial hardware (CAEN and Wiener) as well as control for additional hardware custom devices designed at CERN. For hardware not covered by JCOP,

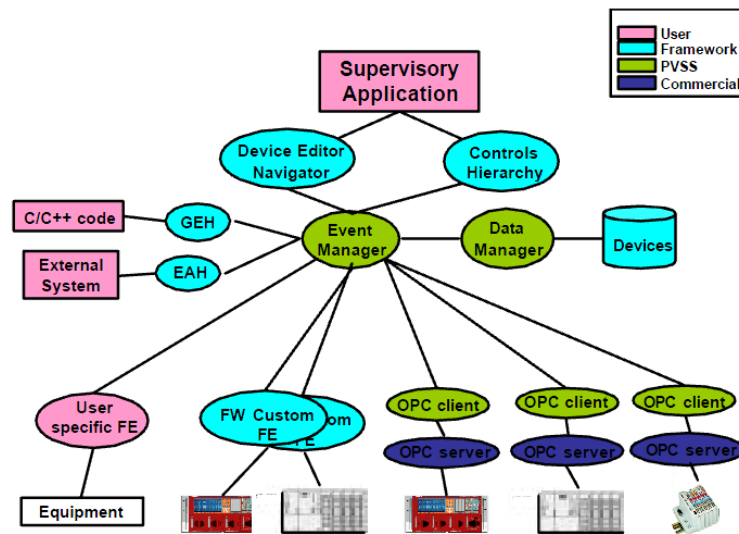


Figure 2.9. Framework Software Components [28].

PVSS offers the possibility of implementing new drivers and components, and CMS has developed sub-detector specific software. The control application behaviour of all sub-detectors and support services are modelled as Finite State Machine (FSM) nodes, using the FSM toolkit provided by the JCOP framework. It is based on State Management Interface (SMI++) [29], a custom language object oriented developed by CERN to control and define the FSM behaviour.

Chapter 3

THE RPC DETECTOR CONTROL SYSTEM

In this chapter the RPC Detector Control System (RCS) [30] is presented. The project, involving the Lappeenranta University of Technology, the Warsaw University, and INFN of Naples, is aimed to integrate the different subsystems for the RPC detector and its trigger chain in order to develop a common framework to control and monitoring the different parts. The analysis of the requirements and project challenges, the architecture design and its development as well as the calibration and commissioning phases represent the main tasks of the work developed for this PhD thesis. This work has required a deep knowledge of the different RPC subsystems (detector, readout, front end electronic and environmental conditions), and their behavior during the different working phases. Different technologies, middleware and solutions has been studied and adopted in the design and development of the different components and a big challenging consisted in the integration of these different parts each other and in the general CMS control system and data acquisition framework. I have been following this project, as main responsible for the RPC Group, along all the operative phases and in the next section I will describe its starting requirements and challenges, the design choices and the development problematic as well as the installation and commissioning phases.

3.1 Mission and Requirements

Role of the RPC Detector Control System (RCS) is to monitor the detector conditions and performances, control and monitor all subsystems involved in RPC operation as well as its electronics. The RCS has to assure a continuous control and monitoring of the detector, the trigger and all the ancillary sub-systems (high voltages, low voltages, environmental, gas, and cooling), required to achieve the operational stability and reliability of a so large and complex detector and trigger system. It has also to take appropriate corrective actions to maintain the detector stability and ensure high quality data, providing also an adequate user interfaces for experts or simple shifters. Therefore, it communicates with external systems such as the databases and the control systems of the accelerator. The working environment represents as well a challenge for the control system because of the high-radiation and magnetic fields environment. In fact the experiment is located in a cavern 100m underground in a not-accessible area during the operation because of the presence of ionizing radiation. Therefore, the control system must be fault-tolerant and allow remote diagnostics. Another main task of the RCS is the control and monitoring of the systems environment at and in proximity of the experiment. These tasks are historically referred to as "slow controls" and include: handling the electricity supply to the detector, control of the cooling facilities, environmental parameters, crates and racks. Also safety related functions such as detector interlock are foreseen by the DCS in collaboration with the Detector Safety System (DSS). Many functions of the RCS are needed at all time. Thus the technologies and solutions adopted must ensure a 24-hour functioning for the entire life of the experiment (more than 10 years). Finally, the RCS should be integrated in the central DCS and Experiment Control System (ECS) in order to operate the RPC detector as a CMS subsystem.

3.2 The CMS RPC Detector

Resistive Plate Chambers (RPCs) are gaseous parallel-plate detectors that combine high time resolution (≈ 1 ns) with good spatial resolution (≈ 1 cm), as already introduced in chapter 1. It makes them as an optimal choice for the CMS muon trigger systems. CMS in fact uses it to identify unambiguously the relevant bunch crossing at which the muon tracks are associated, even in presence of the high rate and background expected (up to 1000 Hz/cm^2). In the next sections, the CMS RPC system design characteristics and operational performances will be described, underlying the requirements and the design

strategies to match the CMS physics requests.

3.2.1 Design Requirements

The RPCs should fulfill some basic specific requirements: good timing, low cluster size, good rate capability. Moreover, they are expected to respond with high intrinsic efficiency and to withstand long term operation in high background conditions. For these purposes, the CMS Collaboration imposed the following requirements on RPC Detectors [15]:

- Detection efficiency $\geq 95\%$ at radiation rates up to 1 kHz/cm^2 .
- Time resolution better than 3 ns and 98% of signals must be contained within 20 ns time windows to allow bunch crossing identification.
- The width of the efficiency plateau $\geq 300\text{V}$ with streamer probability $< 10\%$.
- The cluster size (i.e. the number of contiguous strips which give signals at the crossing of an ionizing particle) should be small (≤ 2) in order to achieve the required momentum resolution and minimize the number of possible ghost-hit associations.
- Power consumption $< 2\text{-}3 \text{ W/m}^2$.
- The intrinsic RPC noise have to be $\leq 15\text{-}20 \text{ Hz/cm}^2$.
- The very front end electronic must be radiation-hard or tolerant to levels of few Gy per year. In addition, depending on the location, a magnetic field of up 1.5 T has to be tolerated.
- Finally, it has been chosen to operate RPCs in avalanche mode, keeping the gas gain relatively low.

3.2.2 Detector Layout

The RPC system is divided in two regions: barrel ($0 < |\eta| < 1.2$) and endcap ($0.9 < |\eta| < 1.6$). It is composed by 912 double gap chambers with in total about 2×10^5 readout channels, covering a sensitive area of 3400 m^2 .

The basic schema of the CMS RPC gap is made by two parallel bakelite plates (1-2

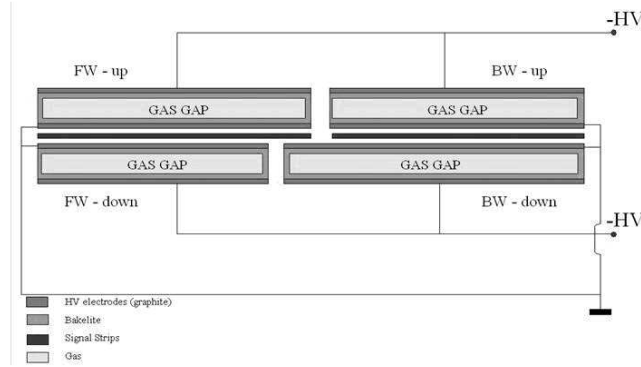


Figure 3.1. A barrel RPC chamber made by two double-gaps and with a strip plane in the middle [15].

$10^{10} \Omega \text{ cm}$) placed at a distance of 2 mm and filled with a gas mixture of 96.2% $C_2H_2F_4$, 3.5% $i - C_4H_{10}$ and 0.3% of SF_6 [31]. The High voltage is applied to the outer graphite coated surface of the bakelite plates in order to have an electric field inside the gas gap, able to generate a charge avalanche along the track of an ionizing particle. The avalanche induces a signal on the copper strips placed outside the gap and isolated from the graphite and connected to the front-end electronic. The gas mixture composition, the width of the gas gap and the operative parameters has been optimized to fulfill the requirements and the CMS operational working condition [32]. A barrel RPC chamber schema, with two double-gaps and a strip plane in the middle, is shown in Figure 3.1.

Barrel In the barrel region, the chambers are located in the iron yoke, strictly following the drift tube system geometry and forming 6 coaxial sensitive cylinders, with the beam pipe as common central axis, as described in Figure 3.2. The layout follows the iron yoke segmentation into 5 wheels, along the axes direction. Each wheel is divided into 12 sectors, housing 4 iron gaps or stations. In the first and second muon stations there are 2 layers of RPC chambers located internally and externally respect to the Drift Tube (DT) chambers: RB1in and RB2in at smaller radius and RB1out and RB2out at larger radius. In the third and fourth stations there are again 2 RPC chambers, both located on the inner side of the DT layer (named RB3+ and RB3-, RB4+ and RB4-). In some special sectors there are four RB4 (sector 4) or one RB4 (sector 9 and 11). In total there are 4 muon stations and 6 RPC layers, hence 480 rectangular chambers, with an average length of 2455 mm long in the z direction, and variable widths from 2500 to 1500 mm,

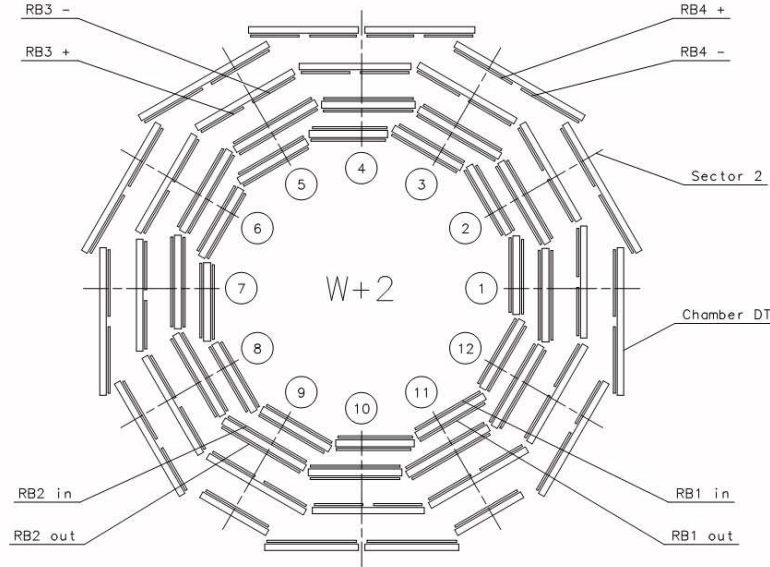
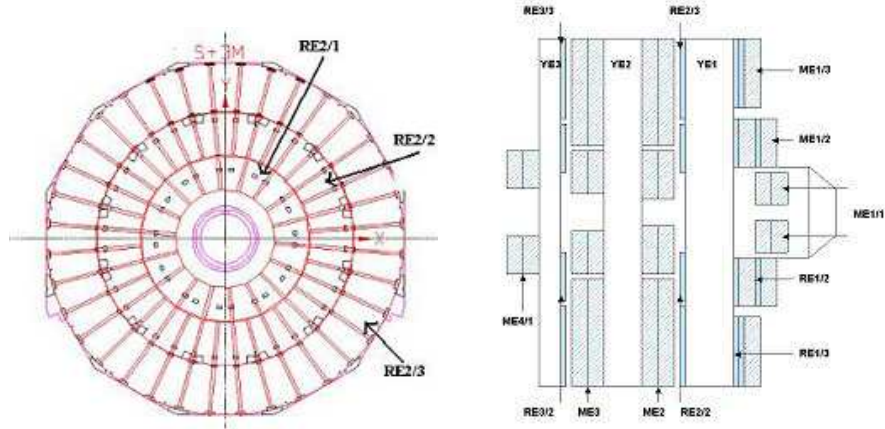


Figure 3.2. Schematic layout of one of the 5 barrel wheels. Each wheel is divided into 12 sectors that are numbered as shown [15].

depending on the chamber type. Each chamber therefore consists of either 2 or 3 double-gap modules mounted sequentially in the beam direction to cover the active area. The strip widths increase accordingly from the inner stations to the outer ones to cover with each strip of different layers the same angle of $5/16^\circ$ in ϕ .

Endcap The RPC endcap system is located, as in the barrel, on the iron yokes. It consists of three RPC chambers layers, for the initial detector, mounted on the faces of the 3 disks in the forward and backward regions, complementing the Cathode strips chambers segmentation. Every station is composed by trapezoidal shape double-gaps chambers arranged in 3 concentric rings as shown in Fig. 3.3a. Except for station 1, the chambers of the innermost ring span 20° in ϕ , all others span 10° and overlap in ϕ to avoid dead space at chamber edges. Station 1 instead is mounted on the interaction point (IP) side of the first endcap disk (YE1), underneath the CSC chambers of ME1, as illustrated in Fig. 3.3b. Strips run radially and are radially segmented into 3 trigger sections for the REn/2 and REn/3 chambers ($n = 1-3$). The 32 strips of the 10° RPC chambers are projective to the beam line. Besides the different mechanical shape and assembly, the frontend electronics, services, trigger, and read-out schemes of the endcap RPC system are identical to the barrel system.



(a) schematic r - ϕ layout of RPC station RE2 on the back side of the first endcap yoke. (b) Schematic layout of the CMS endcap for the initial muon system.

Figure 3.3. RPC Detector Endcap layout [15].

3.2.3 Read-out electronics

Front-End electronics The analog signal induced by the passage of the ionizing particle inside the RPC active volume is produced on the copper strip and then collected by a custom electronic boards, called Front-End Boards (FEBs)[33], attached to the chambers frame. The FEBs are aimed to collect, amplify and discriminate the signal from each strip and then send them unsynchronized to Link Boards (LB), placed on the balcony around the detector. The FEBs house two (barrel version) or four (endcap version) front-end chips, designed with custom ASICs in AMS 0.8 μm CMOS technology. Each chip receives the signals coming from 8 strips and processes them through the following stages: amplifier, zero-crossing discriminator, one-shot, and LVDS driver, as described in Fig. 3.4. The $15\ \Omega$ trans-resistance input stage, adapted to the characteristic strip impedance, is followed by a gain stage to provide an overall charge sensitivity of $2\ \text{mV/fC}$. To assure accuracy to the RPC timing information and provide an unambiguous bunch crossing identification, the zero-crossing discrimination technique was adopted to make it amplitude-independent. The discriminator is followed by a one-shot circuit, that produces a pulse shaped at $100\ \text{ns}$ to mask possible after-pulses that may follow the avalanche pulse. Finally, an LVDS driver is used to send the signals to the LB in differential mode.

Off-detector electronics Once sent to the LBs, the data are synchronized the 40-MHz LHC clock and transmitted them to the trigger boards (TB) located in the CMS counting

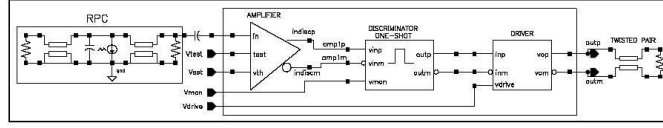


Figure 3.4. Single channel block diagram of the front-end electronics.

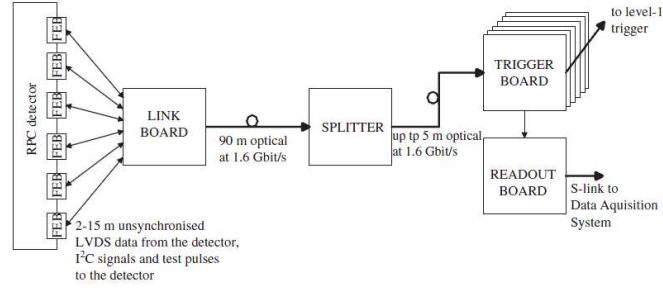


Figure 3.5. An overview of the trigger and readout path of the CMS RPC detector.

room over a 90-m optical link, as shown in the block diagram of Fig. 3.5. The communication with the FEBs is handled exclusively by the LB, thus it takes care of the configuration of the FEB working parameters and the monitoring of their working conditions. On the TB, the data from the links are deserialized and transmitted by 18 parallel buses both to the RPC trigger Pattern Comparator (PAC) mezzanine boards, in charge for the generation of the L1 signal to the CMT, and the Readout Mezzanine Boards (RMB), towards the DAQ chain [34]. The Trigger Boards contain the complex PACT logic which fits into a large FPGA. Since duplicate tracks may be found due to the algorithm concept and the geometry, a ghost busting logic is also necessary. The RPC muon candidates are sorted separately in the barrel and forward regions. The best four barrel and the best four forward muons are sent to the Global Muon Trigger. On the RMB, the data are demultiplexed (selected channels can be masked to avoid duplication of data) and stored in a FIFO memory, awaiting a trigger signal. The data originating from the bunch crossing of a trigger are transmitted via optical links to the Data Concentrator Cards (DCC). Three DCC boards concentrate the optical links from all TBs, each DCC taking data from 36 RMBs.

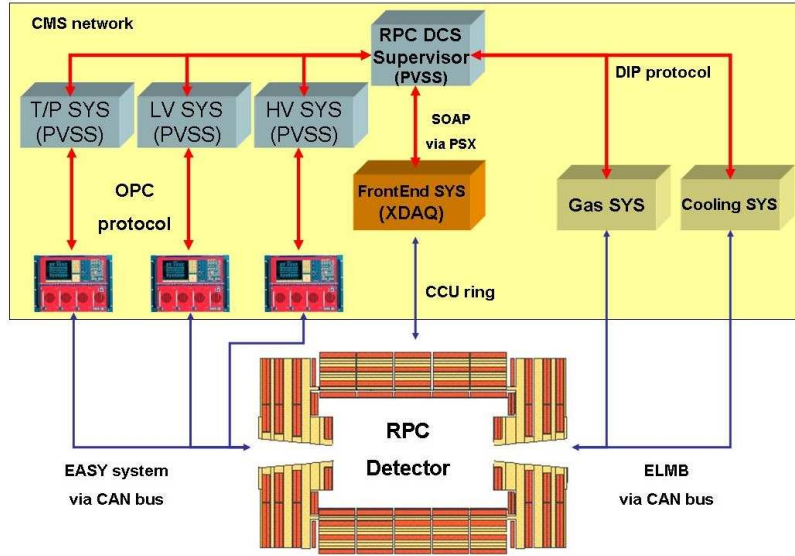


Figure 3.6. The CMS RPC detector control system layout

3.3 The RCS Architecture

The RCS (RCS) is hierarchically organized in a tree-like structure and subdivided in several sub-systems, aimed for different tasks (Fig. 3.6): High Voltage (HV), Low Voltage (LV), environmental (humidity, temperature, and pressure), front-end electronics, gas, and cooling systems, where each component has a certain level of operational independence. The architecture of each sub-system can be divided in the Front-End (FE) equipment, constituted by the hardware components (i.e. sensors, actuator, power supplies, etc) located around all experimental area, and a Back-End (BE) system, composed by the computers network. Because of the large variety of equipment to be controlled, the standardization of the hardware and of the software interfaces is of primary importance for the homogeneous control of all different detector components. It assure the development of a uniform operator interface as well as minimize the implementation and maintenance efforts. Hence for the connection of the BE system to the FE, the industrial buses and protocols are preferentially used, e.g. CAN bus [35] and OPC [36], while some devices are connected custom protocols via Ethernet (DIP, SOAP messages).

In accordance with the CMS official guidelines [26], all RCS back-end applications have been developed using the commercial ETM SCADA (Supervisory Control And Data Acquisition) software, PVSS [27] and the standard Joint Control Project (JCOP) framework

components [28]. Due to the large amount of devices from different subsystems (HV, LV, environment, gas, and cooling), the control and monitoring has to be done in parallel and distributed over different machines. Nevertheless all the subsystems are handled and controlled by the RPC supervisor, aimed to gather and summarize all the information in order to present a simplified but coherent and homogeneous interface to the operators. The different subsystem, their requirements and the design choices will be described in the next sections.

3.4 The RPC Power Supply System

The Power Supply System is in charge to distribute and control the voltages to all the chambers and the equipments involved in the RPC operation. The complexity and the high granularity of the RPC system impose challenging constraints on the development of the power distribution system, particularly considering the hostile environment where they operate. In the muon system, a large part of the power system is located close to the detector and in particular inside the racks placed on the balconies around the barrel wheel and the endcap disk. In this area the magnetic field can reach up to $6 \cdot 10^{-2}$ Tesla, while the radiation is up to 10^7 proton/cm² and $5 \cdot 10^{10}$ neutron/cm² [37]. The power system has been designed taking into account the environmental requirements and the necessity to minimize the probability to have dead or inefficient regions due to the failure of some power supply channels.

Every RPC requires to operate two independent floating HV channels (one per layer) and two independent LV channels for powering up the FEBs. The high voltage lines are aimed to generate the electric field inside the gas gap active volume, whereas the digital and the analogue voltages are required for the FEB chips operation. Different configurations are foreseen between barrel and endcap chambers, choosing a good compromise between the cost and granularity. Every barrel chamber has the two gaps joint together to the same HV channel and two independent LV lines to supply all its FEBs. Being different the chamber size and less its power consumption, the services of two adjacent chambers in the endcap region are joint together in order to have one single HV channel supplying 2 double-gaps, and, from the LV point of view, two independent LV channels for two chambers. Additional low voltage channels are also required to supply Link Boards located on the balconies in the experimental cavern. Hence the entire RPC power system consists of :

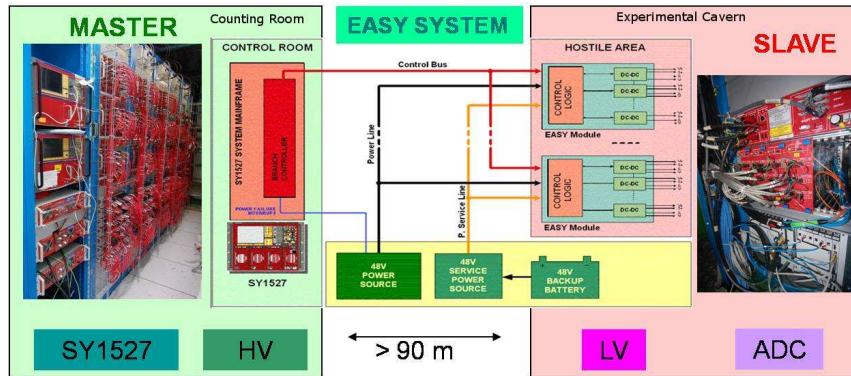


Figure 3.7. Schematic view of the Power Supply System, based on the CAEN EASY Technology.

- 912 high voltage channels,
- $\simeq 1000$ low voltage channels for front end boards on the chambers,
- $\simeq 300$ low voltage channels for the link boards.

CAEN EASY SYSTEM

The solution chosen by the RPC collaboration for the power system is based on the CAEN EASY [38](Embedded Assembly SYstem) project. It consists of components made of radiation and magnetic field tolerant electronics and based on a master-slave architecture. This architecture allows to separate the control part, made by components not-radiation hard, from the supply modules, that can operate in such environment. For the Power Supply System a standard approach has been used, based on modular system where crates and controllers are common, selecting different power supply modules as needed.

The control part in the CAEN EASY technology is accomplished by the SY1527 Main-frame controller, that by mean of branch controllers boards, controls and communicates over a CAN bus with crates located several meters faraway. This master part has to be placed in a safe and accessible area as the electronic room. Two possible configuration can be implemented: one solution is to have the complete power supply situated in the underground electronics rooms, where the environment is safe, whereas the other is to separate the control unit and power module, leaving the former in the counting room and

placing the latter in the cavern close to detector, being based on radiation tolerant electronics. Both configuration are adopted for the power system, as described in Figure 3.7. The second solution has been adopted for the LV system in order to avoid the consequential high large voltage drop and the high current required in case of the 200m long cables. The first configuration is used for the HV system, being the required current $\approx O(6)$ less than LV, in order to easily fix any problem regarding the connection and the distribution of the HV.

In order to fulfill the RPC detector power requirements in Table 3.1, different EASY power supply boards prototypes has been prepared by CAEN and tested at CERN 904 facilities in the last three years. After a testing and optimization phase together with CAEN engineers, a satisfactory board operation has been achieved in term of read-out precision and operational stability and reliability, able to fulfill the RPC community requirements. The RPC power supply system at its startup configuration is composed by 96 EASY CAEN A3009 LV boards for powering up the FEB electronics, 64 EASY CAEN A3016 LV boards for the Link Boards, whereas the HV system instead has 116 EASY CAEN A3512N boards [38]. The latter is designed with an output voltage that can be programmed and monitored in the 0-12 kV range with 1 V resolution and with a monitored current resolution of $0.1 \mu\text{A}$.

Power Supply	High Voltage	LV for FEB	LV for LBB
Hostile Environment	Yes	Yes	Yes
Voltage	12 kV	7 V	4 V
Current	1 mA	3 A	14 A
Programmable Voltage	0–12 kV	0–9 V	0–5 V
Current Precision	0.1 μA	100 mA	100 mA
Voltage Precision	< 10 V	100 mV	100 mV
Trip Settings	0–100 s	0–10 s	0–10 s

Table 3.1. Requirements for the HV and LV system for RPC Chambers

3.4.1 The DCS of the Power System

The control operation on the power system is performed through different levels in a redundant way. First safety mechanisms are implemented directly at the boards level, assuring fast and safe actions. Programmable parameters are in fact available for each

channels to promptly act in case of major problem and bring the detector in a safe condition. Indeed each High Voltage (HV) channel has an absolute (hardware) over-current and over-voltage protection that automatically trips the voltage if any of these parameters exceed the limits. The HV current trip limit is programmable and is usually set to a value lower than the hardware protection. As for the HV, each LV channel contains a hardware protection for the analog and digital voltages and currents at the output of the LV module, tripping the channels in case of the this alarm condition, according to the programmable trip time selected. The other controls are performed at the software level by the back-end applications. The communication with the CAEN power system is managed by the Mainframe SY1527 through the OPC protocol [36], following the schema in Figure 3.8. The software applications based on PVSS are distributed over four servers for resources optimization and loads balancing. The acquisition is based on an event-driven approach and the most significant parameters are handled with a 2 s refresh time.

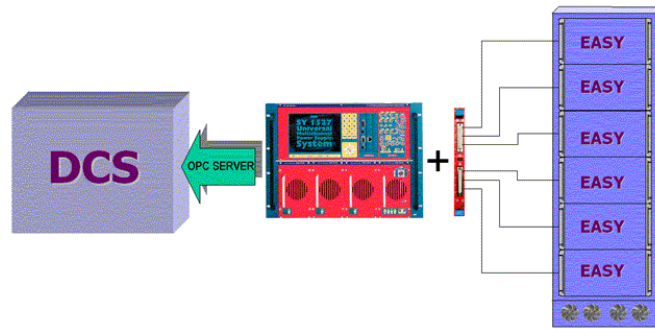


Figure 3.8. The CAEN mainframe can operate independently the power channels and it communicates with the DCS via OPC. The DCS monitors the system status and sends commands to the Mainframe.

The software part is aimed to enhance the hardware level protection by mean of several slower safety checks on each channel, and to provide an easy and robust interface to operate the system. Additional control on the values set, the incoming alarm conditions and the equipment status are performed in order to prevent harmful situations for the hardware. Programmable actions are foreseen to switch off the LV and HV boards or gently rump down the voltages to safer status conditions in case of high working temperature or failure of the auxiliary systems. The DCS is also the interface between the power supply channels and the higher levels of the control system. It handles multiple commands from the supervisory DCS application, translates those into the right sequences of single com-

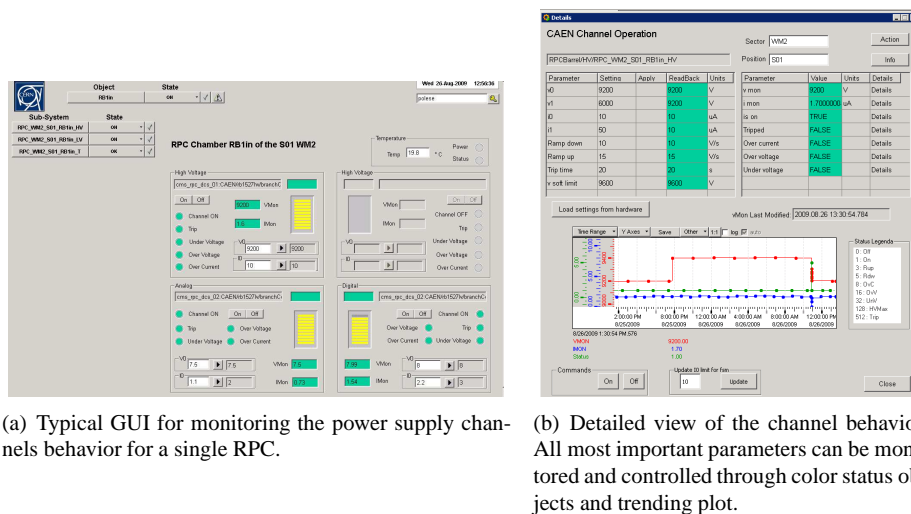


Figure 3.9. RPC Power Supply System GUI.

mands to operate safely and correctly the detector. An specific graphical user interface is also available to the user with a simple interface where monitoring all the most important parameters, the alert condition status and the behavior of the single channels over time 3.11.

3.5 The Environmental Control System

The performances of the RPC detector are strongly related to the operative temperature and humidity since some detector physics parameters, e.g. the noise rate and the dark current of the chamber, strictly depend on them [39]. Hence to assure the quality and stability of the data taking over all the CMS lifetime, a crucial requirement is to provide an homogeneous, high granular and robust sensors network, able to provide a complete view of the RPC status. In the RPC system, several quantities have to be monitored: the gas temperature and humidity, the temperature of the air inside the detector volume, the temperature of the cooling pipes (sensors located at the exhaust of the pipe), the temperature of front-end boards, and the environmental relative humidity. The number and type of the installed sensors in all the RPC system at its start up is described in Table 3.2. The map of the air temperature sensors installed is illustrated in Figure 3.10. Additional temperature probes are also installed on the endcap cooling pipe in some crucial points to have a complete overview of the detector thermic map. The relative humidity sensors are in-

stead installed on the gas distribution racks for each disk and wheel input and output, and on some reference chambers on the endcap disks. They are aimed also to provide early warnings about high humidity conditions that may potentially lead to water condensation inside the detector.

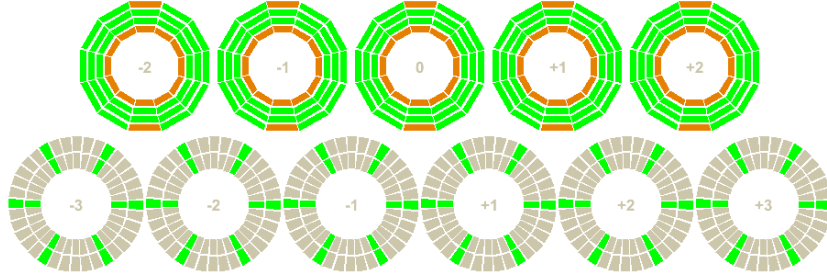


Figure 3.10. Location of the air temperature sensors inside the chamber. In the barrel all the stations (green) are equipped with one sensor but same bigger stations that have two probes (orange). In the endcap region, the sensors are installed only on some reference stations (green).

The temperature sensor is the AD592BN, made by Analog devices, whereas the sensor HIH4000 is used to measure the relative humidity. They assure the robustness, reliability and precision required and can operate in the radiation and magnetic field environment as described in Table 3.3. Both sensors are powered and read by the CAEN ADC (A3801A) boards, equipped with 128 channels and a 12 V input stage. All ADC boards are placed in the balcony around the detector, in the same EASY3000 crates used for LV.

Additional sensors have been installed also on the electronics boards inside the chamber to monitor the working temperate and assure the effectiveness and safety of the working condition. The RPC is equipped with about 7000 front-end boards (FEB) and every FEB has one or two temperature sensors (AD7417) with a nominal accuracy of $0.25^{\circ}\text{C}/\text{LSB}$.

3.5.1 The DCS of the Environmental Control System

The monitoring and control of the environmental information, being read out from the ADCs located inside the EASY crates, are performed via OPC server in PVSS with a 10 s refresh rate. All the values are constantly monitored and protective actions are taken on the chamber hardware in case of high temperature (more then 24 degree) or humidity

Region	Air Temp.	Env. RH	FEB Temp.	Gas Temp.
Barrel Wheel +2	62	-	944	4
Barrel Wheel +1	62	-	944	4
Barrel Wheel 0	62	-	944	4
Barrel Wheel -1	62	-	944	4
Barrel Wheel -2	62	-	944	4
Barrel Total	310	-	4720	20
Endcap Disk +3	12	4	378	4
Endcap Disk +2	12	4	378	4
Endcap Disk +1	12	4	378	4
Endcap Disk -1	12	4	378	4
Endcap Disk -2	12	4	378	4
Endcap Disk -3	12	4	378	4
Endcap Total	72	24	2268	24

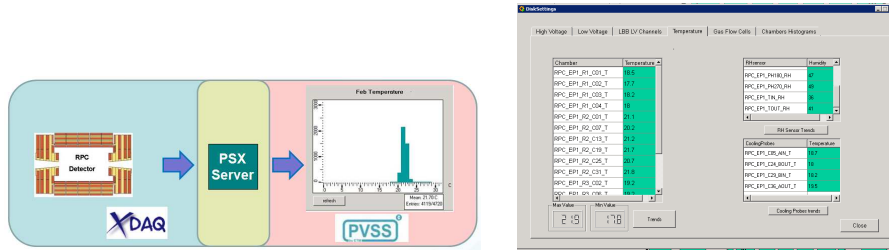
Table 3.2. The number of environmental sensors and their physical distribution.

Environmental sensor	Temperature	Humidity
Hostile Environment	Yes	Yes
Input range	-10°C +60 °C	0–100 % RH
Accuracy	0.1 °C	±2.5% RH

Table 3.3. Requirements for the environmental network for RPC Chambers

(more than 70%) out of the safety ranges. All the information is also available to the users in several panels of the graphical user interface 3.17b in order to monitor the parameters evolution over time and correlate them online with the other detector operation parameters.

The FEB board temperatures are instead read back from the Link Boards, via CCU ring through XDAQ, and then are sent via soap messages to PSX/PVSS, as described in Figure 3.17a. During the normal operation the average data flow measured bandwidth is stably about 2 kB/s. All this information is gathered and controlled by a dedicated PVSS application, able to correlate them and take protective actions, e.g. turn off the power to the problematic FEB, in case of harmful situations.



(a) Building block diagram of the FEB temperature data flow. The information is collected from the LB by a XDAQ application and then sent via PSX to the PVSS application.

(b) Example GUI for monitoring the environmental sensors of a detector region.

Figure 3.11. RPC Environmental Control System.

3.6 The Gas System Monitoring

Being a gas detector, the RPC performances are strongly influenced by the quality and the composition of the gas mixture as well as the working pressure of each chamber, hence a stable and reliable gas monitoring system is a strongly requirement for the correct detector operation. Therefore, the RPC system high granularity and the large area in which it is spread as well as the potentially harmful conditions cause by wrong mixture composition, impose challenging constraints to the gas distribution system network and the design of a high redundant and reliable monitoring system. The CMS RPC gas composition is composed by a non-flammable mixture of 96.2% $C_2H_2F_4$, 3.5% $i-C_4H_{10}$ and 0.3% of SF_6 , plus a percentage of about 45% of water humidity to keep the bakelite resistivity constant. The basic functions of the RPC gas system are to mix the different gas components in the

appropriate proportions and to distribute the mixture to the individual chambers. The large detector volume and the use of a relatively expensive gas mixture make a closed-loop circulation system mandatory [31]. The system consists of several modules distributed along different locations in the experimental area, as described in Figure 3.12. To avoid the usage of flammable gas inside the environmental hall, the preparation of the gas mixture is done in a separate hall in surface. Here the gas is mixed at the proper concentration, humidified, analyzed and then distributed to the gas distribution racks, located around the detector in the experimental hall. The gas mixture is then distributed to the different stations and the relative flows are constantly monitored in order to detect possible leaks. The gas mixture in output from the each station is then recovered, put in recirculation and sent in surface to analyze the impurity level and afterward re-enabled the cycle. Results from long term tests performed by CMS showed that the impurity concentrations produced in the RPC chambers are high enough to influence the detector performance if they are not properly removed from the mixture. Therefore, to achieve a high recycling rate the closed-loop circulation system is equipped with a purifier module containing 3 cleaning agents.

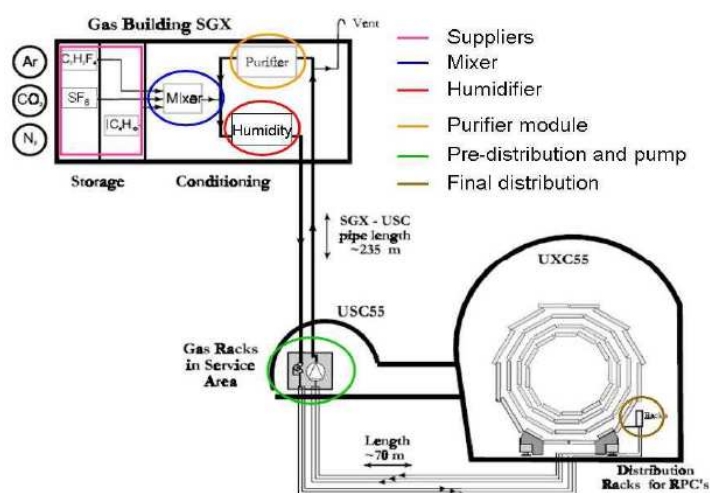


Figure 3.12. Closed-loop circulation system.

3.6.1 The Gas monitoring Applications

Because of the complexity of the gas system and the high level of protection required, the gas monitoring system is built on different levels, both hardware and software, and composed by different projects with different tasks. The acquisition of all the gas system parameters and the monitoring of the entire chain, from the mixing to the chamber, is provided by a CERN centralized system, LHC GCS project [40]. To reduce the effort in the development, maintenance and operation phases, CERN decided to create this project, aimed to provide the Gas control system for all the 4 LHC experiments. As the process to be controlled is very industry-like, it has been decided to use industrial tools and principles. It is based on Schneider Programmable Logic Controllers (PLC), Profibus, CAN and a library (UNICOS) to develop applications in both PLCs and PVSS. The hardware level control is performed via PLC, allowing to take easy and protective actions promptly. For example in the RPC gas system such facility is used to control the gas mixture and keep it non-flammable. As soon as the $i - C_4H_{10}$ fraction increases beyond the flammability limit, the PLC takes care of stopping the flow through the detector and cutting off the voltages applied to the chambers. Similar actions on HV chambers are foreseen in case of main failures on the gas distribution lines. All the sensitive parameters acquired by the CGS are shared also with the RCS via DIP Protocol. Information like the gas quality and the mixture composition, the chambers input and output flows as well as the actual status of all the equipments involved in the preparation and distribution of the gas mixture, are monitored in the RCS and used to operate safely the detector, allowing to take action on the other relevant hardware components depending by the gas behavior. It also allows to correlate this data online with other operational parameters in order to optimize the detector behavior. A typical GUI panel to monitor the gas system information is illustrated in Figure 3.13.

To check the quality of the gas composition and the purifier effectiveness and to spot promptly any saturation effects, the RPC Collaboration has developed two independent and complementary projects, aimed to continuously monitor the mixture: the gas quality monitoring and the gas gain monitoring. The gas quality monitoring system [41] will perform both qualitative and quantitative gas chemical analysis with a set-up which includes gaschromatograph, pH sensors and specific fluoride electrodes, in order to continuously monitor the status of the recirculation and to detect a wide range of pollutant produced during the detector operation. The gas gain monitoring system [42] is composed by a set of small single-gap RPCs, located in surface, supplied with the same gas mixture. They allow to monitor the work point of the gas mixture used by means of gas gain and effi-

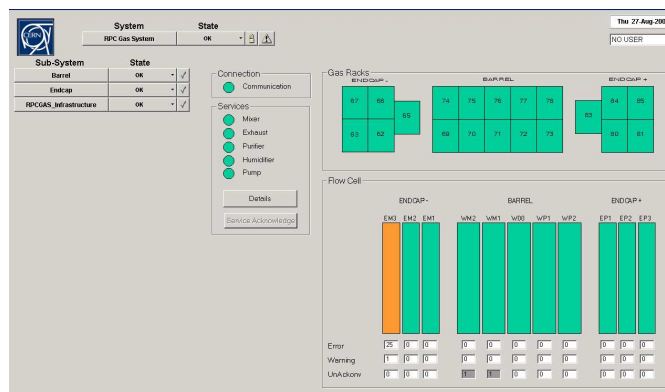


Figure 3.13. The Main Gas Monitoring Panel from where it is possible to monitor all the relevant parameters involved in the RPC operation.

ciency scan at different high voltages in order to provide fast and accurate determination of any shift in the working point operation.

3.7 External Control System

As External Control System are referred the other control systems that have their own independent control and with which the RCS has to interact. Although these systems are designed to react in case of problems, early indications of their status must be notified to the RCS since they may have consequences onto the detector and automatic corrective actions, driven by the DCS, may be required. The cooling and DSS system will be presented in the next sections, being deeply involved in the RCS operation.

3.7.1 Cooling and Ventilation

The temperature has influence on the stability of the mechanical structures of the detector, on the response of the detecting elements, and on the electronics lifetime and safety. Hence an efficient cooling system is a mandatory requirement for an efficient and robust operation. Cooling and ventilation is an infrastructure service provided by CERN for all the LHC experiments. During the CMS operation, the total amount of heat dissipated in the experimental cavern is about 800 kW, that needs to be intercepted by the cooling

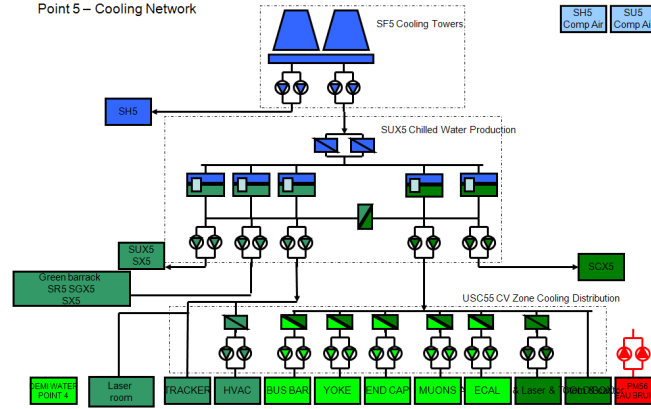


Figure 3.14. CMS cooling plan. The RPC chamber are cooled by different lines, to keep stable the chamber electronics temperature and to avoid heat exchange from the other subsystems.

water at 18° for the Calorimeters and the Muon systems and by C_6F_{14} coolant, used in the Tracking system. A description of the CMS cooling plan is shown in Figure 3.14, where the different supply lines for the different regions and different subsystems are underlined. In addition, the cooling system has to keep at safe temperature the hardware equipments like the rack system and the DAQ server network. Crucial parameters such as flow rate, temperature and dew point, are monitored via DSS in several point of the distribution chain in order to have a detailed overview of the system status and detect eventual loss of coolant. This information is of primary importance for the RPC detector and are used inside the RCS to take automatic and protective actions on the hardware involved in case of problem.

3.7.2 Detector Safety System

The Detector Safety System (DSS) [43] cooperates with the DCS for the experimental area safety, taking care of the experimental equipment protection in case on major hazards, like smoke, fire, flammable gas, oxygen deficiency. This kind of harmful conditions require a level of operation that cannot be accomplished by the DCS because of its complexity and high granularity. The DSS is instead designed to be simple and reliable and consequently its actions have to be fast and quite coarse, e.g., cutting the power to the entire cavern in the case that smoke is detected. DSS actions thus will in general disrupt the data taking, but avoid damage to experimental equipment and consequential long in-

interruptions. All alarms of the DSS are transmitted to the RCS and are used to execute predefined control procedures. For specific DSS harmful situations involving the RPC detector in which a very fast action is not required, a few minutes delay in the DSS action execution is foreseen in order to execute more gently shut-down procedures before that the DSS switches off the equipments. To fulfill its requirements, the DSS system has to be based essentially on hardware components. The front-end is a redundant array of two PLCs, that interpret the signals coming from the connected sensors according to a programmable alarm-action matrix. Actuators, attached to the output of the PLCs trigger actions. The PLCs are scanning all input channels, processing the alarm-action matrix and modifying the state of the outputs accordingly. Such a cycle will take about 500 ms, allowing the DSS to react to any hazardous situation with a response time below one second.

3.8 The RCS Supervisor

All the control subsystems described in the previous sections are able to work as stand-alone component and participate the general RPC system operation, each covering a particular task. To gather all the information and to present a simplified but coherent and homogeneous interface to the operators, a supervisor level is required for the correct operation. The main aim of the RPC Supervisor is to summarize the status of all the sub-systems involved in the RPC operation and present it to the central DCS, defining the operative conditions for data taking. It uses most of the functionalities provided by the JCOP+PVSS software, such as the finite state machine, the graphical user interface, the alarm handler and the ORACLE database interface, that allows the storage of the data in the CMS online database and the loading of the hardware configuration from the CMS configuration database. In the next sections its different functionalities and the design solutions are presented.

3.8.1 Architecture

The huge amount of components under the RCS control and the high granularity of the system require to describe it in a hierarchical way. The RCS software architecture has in fact been developed following a hierarchical double-tree structure: a geographical and a hardware oriented tree (Fig. 3.15). Both trees give useful information on the system

from different points of view. The status of the equipment involved in the operation is described through the hardware tree, useful to find out and handle problems occurring in a particular hardware component, involving several detector parts. The geographical tree, instead, describes the system from the detector point of view, focusing on the location of the each component on the detector. This subdivision closely follows the geometry of the detector, i.e. wheels and sectors for the barrel, discs and rings for the endcap, allowing a close correlation with readout data. PVSS and JCOP framework allow an easy implementation of such a structure. Every tree node is described by predefined objects, Control Unit (CU) and Logical Units (LU) that, with different task and privileges, are aimed to drive the behavior of the hardware equipments and subsystems under them. In fact they can configure, monitor, and control all child nodes and recover from error state. This facility assures the partitionability and scalability, allowing a robust and powerful management of the system. At the lowest level, as leaves of the tree, there are different logical groups describing the hardware devices: HV, front-end LV, trigger LV power supply, and environmental systems. These tree nodes, representing electronic channels, are described instead by Device Units (DUs). Each DU is the interface to the hardware component; it translates the received commands, understands the device states and generates eventual alarms. The HV and LV channels, the power supplies, and the slave crates are managed separately through dedicated DUs. The root (top) node of the RCS is connected directly to the CMS central DCS system and is used to communicate and exchange actions, states and commands. The commands, coming from the central DCS, are propagated through the RPC FSM tree, down to the devices. Here they are interpreted accordingly as hardware commands. The hierarchical tree structure allows only vertical data flow: commands move downwards, while alarms and state changes propagate upwards (Fig. 3.15).

3.8.2 The Finite State Machine

In order to fulfil a high rate of automation in control processes, reduce human errors, unavoidable in repetitive action, and optimize recovery procedures in case of undesired states, all the RCS hierarchy nodes are implemented through a Finite State Machine (FSM) mechanism. It offers an easy, powerful and safe way to get the full detector control, through the definition of a finite number of states, transitions, and actions. It allows to summarize the detector status through a limited number of states, drive it to predefined configurations and translate all the operation modes in simple actions, hiding to the operator the complexity of the actions required. The FMS toolkit in PVSS is based on SMI++ [29] and provided by the JCOP framework. It allows thus to map the complete hardware

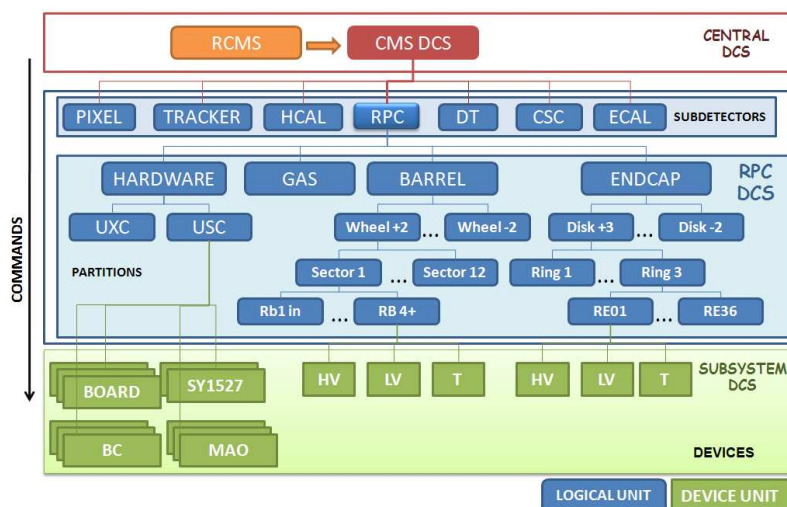


Figure 3.15. Structure of the hierarchy tree of the RCS. Different branches describe the RPC system from geographical and hardware points of view. All commands go down the hierarchy, while information and error messages are reported upwards.

onto a hierarchy of FSM nodes and implement the structures and the procedures to correctly operate them by means of an object-oriented approach, where the programmable behavior of the FSM units are defined in FSM object types. In order to be able to operate different detector parts independently, individual SMI domains can be separated from the control hierarchy. Further, the partitioning capabilities of the FSM toolkit allow operating parts of the hierarchy in distinct modes. Device-oriented FSM objects can be detached from the tree (“Disabled”) such that they do not propagate their state nor receive commands. The FSM layer has a detector oriented hierarchy and it hosts more than 2000 FSM elements interlinked. This software layer hosts more than 5000 control loops to guarantee a safe and automatic detector operation.

The states and the commands for the top nodes as well as the conjunction nodes have been chosen by CMS in order to have a uniform structure. The states are: ON, OFF, STANDBY, and ERROR and the commands are: ON, OFF, and STANDBY. The use of these particular states and commands ensures uniformity and compatibility with the central DCS, permitting adequate transitions between the states. Their small number and general definition makes them suitable for all sub-detectors. A typical device state model defined for a HV channel is described in Figure 3.16: all the feasible channels configurations are described by states and the transitions from one state to another are handled via predefined steps that assure correctness and reliability to the operation. In each step the

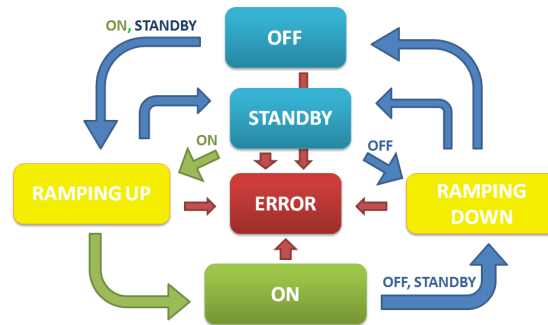


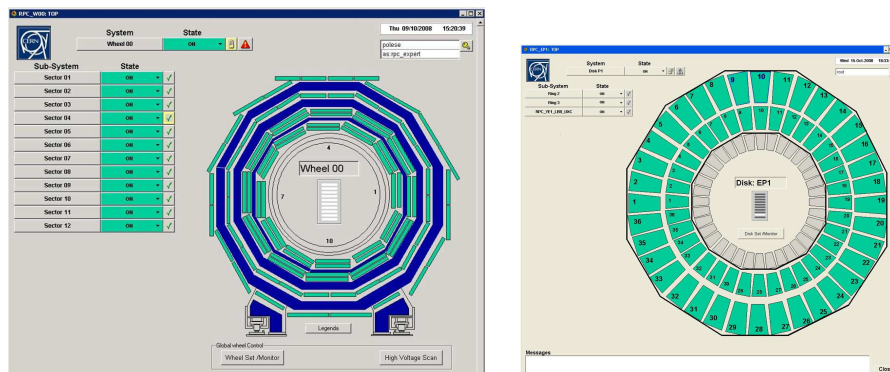
Figure 3.16. Structure of the hierarchy tree of the RCS. Different branches describe the RPC system from geographical and hardware points of view. All commands go down the hierarchy, while information and error messages are reported upwards.

FSM takes care of loading from the database the right values to apply and alarm settings. The states from central DCS are translated in meaningful states for RPC. For this reason a transitional state (RAMPING) has been added to the previous states. It describes the situation in which the high voltage of one or more chambers is ramping up or down. The STANDBY state is used for the RPC detector as a safe state in which the LV channels are ON, while the high voltages are at an intermediate and safe value. This state has been implemented for test and calibration runs or for period with a “not stable” beam and magnet ramping conditions.

3.8.3 The Graphical User Interface (GUI)

The GUI is developed to be an intuitive tool to control and monitor the detector, easy to use also for non-experts and able to protect the system from any dangerous action. It is a collection of panels in PVSS language and offers the following functionalities:

- an easy navigation throughout the entire system structure, thanks to a combination of text, graphical objects and synoptic diagrams;
- visualization and setting of any process variable;
- global parameter setting, thus speeding operations and reducing human errors;
- plots, diagrams, histograms, and tables for a first online analysis of the detector behavior;



(a) A barrel wheel panel of the Supervisor DCS. All the object are colored according the status of the chamber.

(b) An endcap Disk panel. Clicking on each chamber is possible to obtain more information about the services status and check the behavior over time.

Figure 3.17. Typical layout of the Supervisor system.

- complete visualization of the alarm condition on all critical elements.

To fulfill the above functionalities, approximately 40 panels (tree structure) have been designed following the naming conventions and the color codes decided centrally by the CMS DCS group. Examples of RCS panels are shown in Fig. 4.13. Here the general states of the different data sources are color-coded and the current readings of the operational parameters are also shown in the panel. The GUI allows a complete control of the entire RPC system and therefore, to prevent any human error, a different access levels have been set. Access Control (AC) for different control aspects within RCS is provided by a set of tools restricting access to the control interfaces to authorized users. Same specific actions that require the expert supervision, are also restricted to the normal operator in order to avoid unsafe operation on the system. The following self-explanatory groups: PVSS expert, RPC expert, and RPC user have been successfully tested during our pilot runs.

3.8.4 Alert Handling

During detector operation, any problem occurring must be detected, signaled and possibly automatically recovered from. On the individual device or channel level, the PVSS alarm mechanism is used to report any abnormal value of a single monitored parameter. An alarm is issued every time the system unwontedly leaves the desired state or if a given

parameter deviates from a predetermined range. A sets of alarm conditions severity levels and recovery procedures have been defined and implemented for all the critical hardware parameters in order to have a very fast alert of any abnormal condition. A Warning severity level is raised for example in case a parameter overcomes out of the safe ranges, but its condition doesn't prevent the normal operation. It warns the operator to investigate the problem in order to avoid forthcoming malfunctions and an eventual interruption in the operation. More higher severity levels are used in case the problem may cause the interruption of the operations or eventually cause implications for other systems. To avoid the accumulation of a large number of alarms on the user interface, summary alerts are foreseen for grouping the most sensible parameters and organized in a hierarchical structure, strictly following the FSM architecture. The RCS alert are handled by the operator through a dedicated GUI and all the most sensible conditions are connected to the external server in charge of warning the proper experts remotely via SMS (mobile "text messaging") and emails.

3.8.5 Integration in central DCS and Run Control

The RCS is directly connected with the central DCS and seen as child in the Central DCS hierarchical structure. In this way the central DCS propagates commands to it and can retrieve alarms and messages directly from the RCS, publishing the RPC status condition to the CMS Run Control during the data taking, according the diagram illustrated in Fig. 3.18.

This bidirectional communication between the RCS and run control allows to synchronize the status of the detector with the physics data taking operation. Moreover, The RCS is also able to operate in standalone mode in order to be used during the commissioning and calibration phase, by means of a direct connection to the RPC Run control. This connection allows to synchronize the configuration operations among different RPC parts, check the status of the entire RPC system and manage centrally the warning and error messages coming from different RPC partitions.

3.8.6 DCS Configuration

The hardware description and the configuration of the RPC system are particularly laborious, due to the large number and heterogeneity of the elements, and require data base

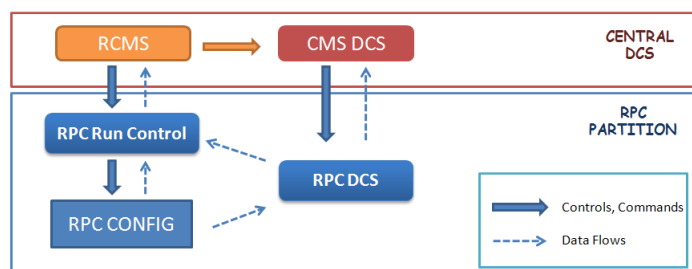


Figure 3.18. Logical layout RCS with other DAQ subsystems.

infrastructures to keep track of the different running configurations. The RCS configuration database is designed to manage the setting of the detector and DCS parameters (such as calibration constants, voltage settings, and alarm thresholds) depending upon the operation mode. All the structural information, geographical position and configuration parameters necessary to put the detector in running condition, are stored in the RCS configuration database, based on the ORACLE technology. A “Configuration” contains sets of devices with their static properties, for example HW addresses, archiving settings, required to recreate the system from scratch. The values to set for the different working conditions, are instead set in “Recipe”. It is a set of values that are run-time specific, such as set points for output channels and alert thresholds, which may change depending on the detector operation mode. This method allows different configurations to be stored as “recipe” for different conditions (e.g. for stable beam, cosmics). Online changes to the configuration parameters can be made via the DCS interface and uploaded to the Oracle database. The configuration data can be used within offline reconstruction and analysis routines independent from PVSS.

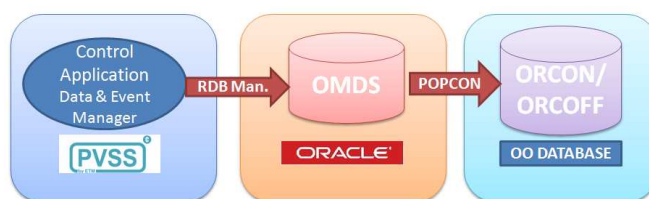


Figure 3.19. Flow of data through the archiving chain from the PVSS application to the Offline database.

Parameters	DeadBand
Chamber Dark current	0.3 μ A
HV Voltage	10 V
LV Voltage	0.1 V
LV current	0.2 A
$T_{chamber}$	0.3 $^{\circ}$ C
$T_{cooling}$	0.3 $^{\circ}$ C
Chamber lines gas Flow	0.5 l/h
Relative humidity	5%

Table 3.4. Deadband used for the most important parameters to store the values in the online database

3.8.7 Condition Database

All the information regarding the running conditions and non event data controlled by RCS needs to be stored in order to monitor the system behavior over time. In particular, the currents and voltages on all the chambers of the system will be constantly read out and stored, together with the environmental conditions, to give a first glimpse of the chamber performance. Therefore, the data processed by PVSS coming from the gas system, the cooling network and the electronics is stored in the same way. This information allows the optimization of the working condition and the study of the equipments response during different phases of the experiment and is useful to understand the ageing behavior of the detector. Because of the huge amount of data monitored, a reduction of the data volume is necessary, to avoid filling the disk space with values due to noise fluctuations. Consequently, “deadbands” are specified for all relevant parameters (Table 3.4), optimized respect to the hardware accuracy and values are written to the database only when new values are measured outside the deadband. In the final configuration the amount of RCS data stored would be about 10 GBytes per year, almost 1/200 of the monitored information. The biggest part of these data is represented by chamber dark current. The interface between PVSS and the different databases is handled through a dedicated PVSS manager for ORACLE DBs, able to assure reliability, redundancy, and stability of the storage system. The information are stored from PVSS to the CMS Online Master Data Storage (OMDS), used by all the online subsystems. Part of these data, useful for detector performance studies and analysis and reconstruction, are processed and stored in the Offline database by a dedicated application PopCon, (Populator of Condition Objects), aimed to store data in an object format that best matches the object oriented paradigm for C++ programming language used in the CMS offline software, as illustrated in Figure 3.19.

Chapter 4

THE COMMISSIONING AND CALIBRATION

4.1 CMS Global data taking

Several are the milestones reached in the last three years to make CMS an unique, highly efficient, and reliable detector. Since summer 2006 different global data taking campaigns with parts or all the subdetectors integrated has been performed in order to learn how to operate simultaneously all CMS subdetectors, the trigger, and DAQ chains as a unique system. These runs represented a very useful experiences for the detectors as well as for the data analysis structure commissioning. From the detectors point of view, the main global run aims are to complete the CMS commissioning, evaluate the efficiency and eventually repair faulty channels, and to check the resolution and improve the detector performance measuring calibrations and alignment constants. On the other hands, the integration and commissioning of the data acquisition and trigger systems and other online tools such as the detector control system and data quality monitoring as well as the testing of the full data handling are important tasks fulfilled during the global run. The different stages and the most important CMS milestones are illustrated in Figure 4.1.

The first global commissioning has been performed in the surface hall during August-November 2006. The main goal of this campaign, called the MTCC (Magnet Test and Cosmic Challenge) [44], was to fully test the solenoid magnet while the experiment was still located in the surface assembly building. As a part of the exercise, a vertical slice of

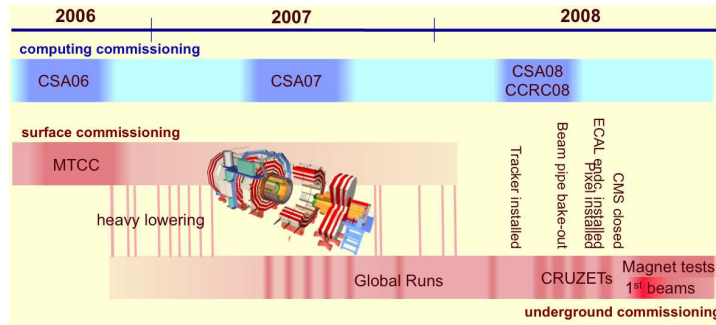


Figure 4.1. Overview of global CMS commissioning activities.

most important detector components (pilot silicon tracking system, ECAL, HCAL, barrel and endcap muon chambers) was operated to record the cosmic ray signal with and without the magnetic field. It demonstrated to be fully operative and able to reach stably the nominal value of 4 T. After collecting about 200 million cosmic muon events, the central detectors were removed and the field maps for different field values measured. The data collected during the MTCC provided an important feedback for the calibration and alignment procedures. The behavior of the detectors in the magnetic field was verified by comparing their performance with and without field and was checked with the simulations. In this sense, the MTCC represented a first global commissioning test of the CMS at all levels, from the data taking up to the physics analysis. Soon after the central heavy elements of CMS have been lowered into the experimental cavern, a series of centrally driven data taking efforts, called “Global Runs”, was performed with a duration of a few days and with an increasing number of subcomponents integrated as soon as the ongoing detector installation and local commissioning activities were completing. Starting in 2007, several cosmic rays runs without magnetic field were performed, with the detector partially opened, for a total of more than 300 million events collected.

In August 2008 the detector was ready and protons circulated in the LHC ring in September. Several event types were collected during the first beam days: beam halo events (mostly muons coming parallel to the beam axis) and beam splash events (when a single beam of $2 \approx 10^9$ protons was dumped on the closed collimators 150 meters upstream). These events contain horizontal particles, useful for forward detectors commissioning and in particular the splash events delivered large energy deposits in the calorimeters. After the LHC accident on the 19th of September, the CMS experiment was kept closed and a long cosmic run at nominal magnetic field was taken (called CRAFT, Cosmic Run At Four Tesla). CRAFT collected 290 million events at 3.8 T magnetic field, out of which

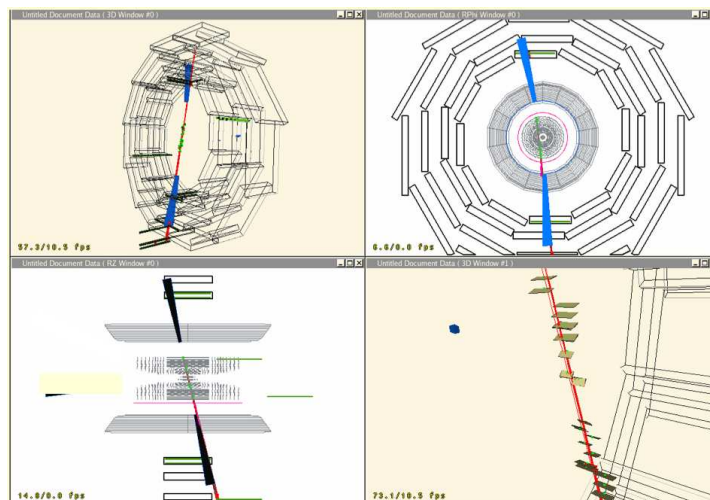
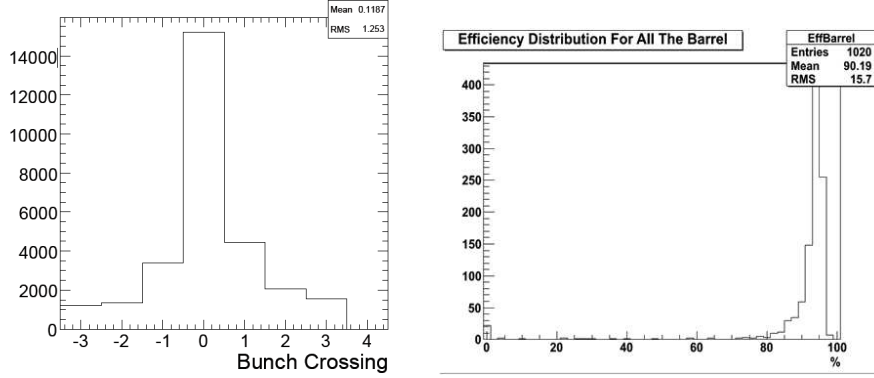


Figure 4.2. Event display showing a global track reconstructed from a cosmic ray signal in the silicon tracker and muon chambers associated with the calorimeter signal.

87% have a muon track in the muon chambers, 3% have a muon track with tracker hits and 30000 events have pixel hits. A typical event with a cosmic muon traversing the whole experiment is shown in Figure 4.2.

4.2 RPC Performance and Calibration

Since the MTCC, the RPC detector has participated to the CMS global runs with a increasing percentage of system integrated, reaching its final configuration during the CRAFT09. They allowed to achieve the commissioning goals and to validate the detector response and performance in its final configuration, demonstrating it matches the CMS requirements. A first crucial point for the RPC system is the synchronization of all the chambers readout inside the apparatus and its electronics, fundamental to satisfy its role of trigger detector. Signals coming from different regions of the detector arrive to the readout electronics at different times due to time of flight, time of propagation along the strip and different cable lengths. In order to get the maximum efficiency, all the signals should be collected in the same bunch crossing interval. Cosmic rays data have been used to synchronize in the best way all the chambers signals and the RPC trigger response with respect to the other triggers. A very good synchronization level has been reached with this data for the barrel, as illustrated in figure 4.3a. For the endcap regions more data is



(a) Synchronization of RPC data: amount of data in a BX as a function of delay to the CMS trigger BX. A peak in the central bin corresponds to data aligned with trigger.

(b) A typical distribution for a CRAFT09 run with all the barrel chamber high voltage at 9.3 kV and FEB threshold 230 mV.

Figure 4.3. The Calibration procedure done during the CRAFT09 data taking period.

still required to achieve the same confidence level, due to lower efficiency of the cosmic rays as probing source for geometrical reason.

After the synchronization, the performance of the detector, in term of efficiency, cluster size and noise, have been studied making use of the interplay between DT/CSC muon system and RPCs. Barrel RPCs can be studied by making use of the local reconstruction of the DT hits at chamber level. The extrapolation of DT segment on the RPC plane gives the possibility to study the RPC performance at local level. For every extrapolation on the RPC surface, RPC fired strips are checked in a small region around the impact point (± 2 strips). Although with a rough precision the RPCs are a position detector. Contiguous fired strips on the same RPC plane are merged together to define a cluster. The cluster size is the number of fired strips of the cluster generated by a crossing particle. The results obtained in terms of efficiency are still preliminary due to the random arrival time of the cosmic rays that could arrive off time on some RPC layer, and to the still-not-optimized signal threshold and working voltage. The method to estimate it for each chamber is described in the next section. A typical distribution for a CRAFT09 run with all the barrel chamber high voltage at 9.3 kV and FEB threshold 230 mV is illustrated in figure 4.3b, where the average value is $> 90\%$.

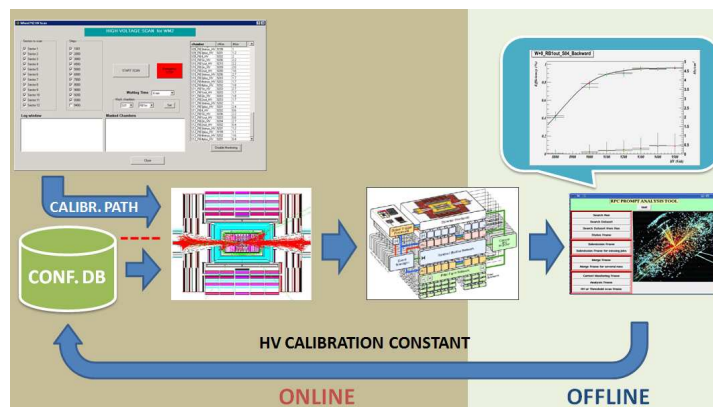


Figure 4.4. Calibration Flow

4.2.1 RPC working point calibration

The detector calibration is an important task to fulfill during this first CMS phase with cosmic rays run and an important rule for it plays the synchronized operations between the online and offline tools. The definition of the best working parameters, e.g. operating voltage and FEB thresholds for each chamber, is crucial to achieve the best performance and is done scanning the detector performance response at different working conditions. RPC detection efficiency is in fact studied taking data at different applied High Voltage and estimating the maximum efficiency for every double gap RPC of the system. The RPC is considered efficient if at least a fired strip has been found at a distance of ± 2 strips respect to the impact point extrapolated from the DT/CSC segment. The calibration flow for such parameters is illustrated in Figure 4.4. The configuration data is stored inside the config db, where the optimized parameters are defined by mean of recipes.

In order to redefine such constants and upload a new configuration inside the database, a HV scan tool is available in the RCS. An example panel to perform this operation is illustrated in Figure 4.5. It offers the possibility to ramp safely the voltages for each chamber through different steps automatically, while the detector response is read out by the DAQ chain at the different conditions. In fact to evaluate the optimal working voltages, at each applied voltage step the efficiency chamber by chamber is estimated. In Figure 4.7 the curve of efficiency as a function of the applied high voltage is shown for a reference chamber. The chamber behavior can be fitted by mean of a sigmoidal function

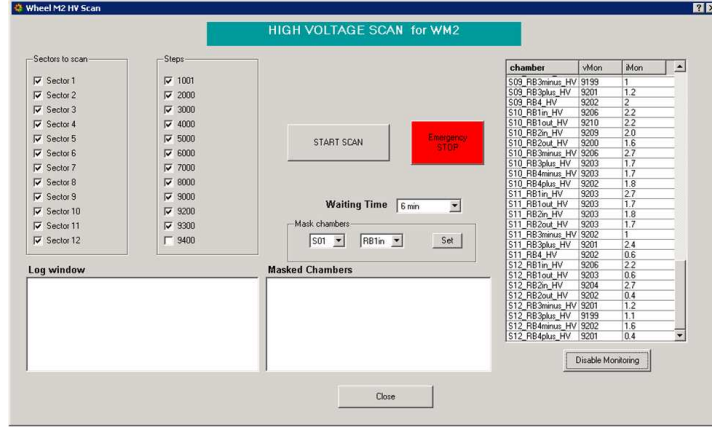


Figure 4.5. GUI for a barrel wheel HV scan procedures.

to each curve using the following parametrization:

$$\epsilon = \frac{\epsilon_{max}}{(1 + e^{-Sl \times (HV - HV_{50})})} \quad (4.1)$$

where ϵ_{max} represents the plateau value of the efficiency, Sl is related to the slope at the flecion point of the sigmoidal function, HV is the high voltage value at which the efficiency reaches 50% of its maximum value and HV is the operating voltage. At each voltage step, the data is thus acquired from the detector and analyzed by the prompt analysis tools to estimate the efficiency chamber by chamber, as described in the Figure 4.4. The RPC operating voltage depends also on environmental parameters [39] such as gas temperature (T) and pressure (P), according to:

$$HV_{eff} = HV \times \frac{P_0}{P} \times \frac{T}{T_0} \quad (4.2)$$

where HV is the power applied voltage, HV_{eff} is the effective voltage relevant for the charge avalanche process across the gas gap, T_0 and P_0 are reference temperature and pressure respectively of 293° K and 1010 mBar. Both parameters are acquired by RCS and transmitted offline to be used in the calibration procedures. The high voltage scan is usually based on at least four HV values to allow a good fit to the data. Once the procedure is ended, the estimated working point for each chamber is calculated by the prompt

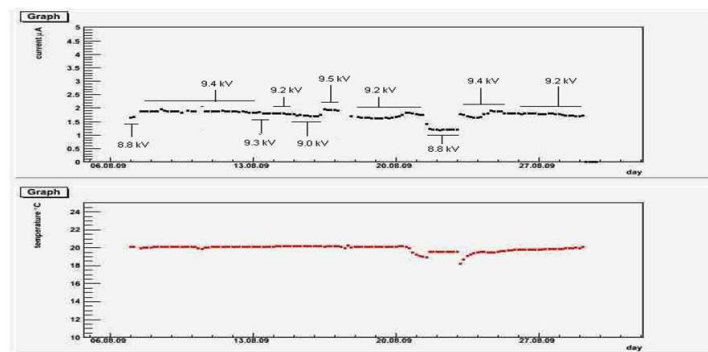


Figure 4.6. Detector calibration procedure. The upper plot describes the evolution of the average voltage applied over time, the lower one shows the behavior of the chambers average temperature for the same period.

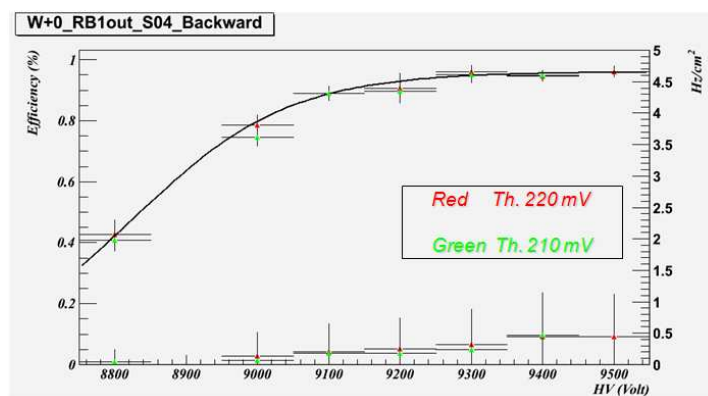


Figure 4.7. Typical curve of efficiency vs applied voltage used to estimate the working point.

analysis tools fitting the efficiency information. The HV operational point so calculated is then stored in the configuration db in a recipe run and loaded and applied by the RCS to the actual configuration. A typical calibration run is described in Figure 4.6, that were performed during the CRAFT09. During the procedure temperature and humidity were monitored via RCS (Figure ??) and recorder in order to estimate the relative corrections on the data to the effective voltage applied on the chamber. The result of this calibration campaigns are shown in Figure 4.8, where the best parameters in term of HV applied and FEB thresholds are underlined.

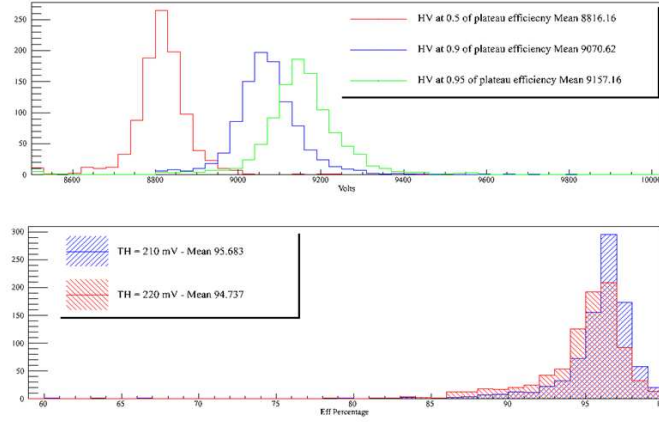


Figure 4.8. Distribution of efficiency as extracted from the fit to the sigmoidal function at different voltages (top) and for different FEB thresholds (bottom).

4.3 The RCS performance during the CMS global runs

The RCS was extensively tested during the hardware installation phase and already used during the commissioning phase as official tool for operating the RPC chambers. The use of the RCS in the RPC commissioning phase was not only important for the operation and safe running of the detector, but also to validate the system itself and to optimize the performance and scale it up. The first significant tests with the real hardware have been performed during the MTCC in the summer 2006, where the RCS has been operated on 5% of the final configuration of the power systems, CMS DAQ software, data quality monitor (DQM), and integrated in the central DCS. During the last three years the RCS has been scaled up with the increasing RPC system complexity and the new hardware installation, including more subsystems as soon as they became available. In the summer 2008 as soon as the installation of the last endcap chambers and their services have been completed, the RCS reached its final hardware and software configuration foreseen for the CMS start up phase. All this information acquired by PVSS is stored in the condition database and then transferred to the offline db to be used in the offline analysis of the detector and trigger performances. In the next section, I will present a selection of the data collected for the qualification of the system, underlying the performances of the crucial systems during the operation and the tools developed to perform such analysis.

4.3.1 RPC Detector Performance analysis tool for not event data

The most important parameters data is stored in the online database as discussed in the previous chapter. This information can be used to study the detector behavior in order to analyze and tune the detector performances inside the online framework. As illustrated in Figure 4.9, the RCS represents the first place where perform a prompt detector physics analysis. From the GUI is in fact available for the users several online histograms and plots over time for the most sensitive detector parameters acquired via RCS, as well additional trends to correlate among them online. Being the RCS focused and optimized on the control and the safety of the detector operations, a more powerful dedicated framework has been developed by CMS in order to allow a more complete and deep analysis, based on standard analysis libraries. The information inside the online database can be in fact acquired and analyzed through the CMS official Web Based Monitoring (WBM) [45], aimed to handle the communication with the OMDS and to run fast algorithm for data analysis. Based on a common web browser interface, the system makes use of a Tomcat server by mean of servlets that interacts with the database via JDBC calls and renders web pages on the client side. As main responsible for the RPC WBM project, I developed together with the WBM team a detailed RPC-oriented GUI, using web based technologies and Java libraries, able to perform a standard analysis on these data and to describe the detector status and help the user to spot easily problems through color coded maps, synoptic diagrams and tables, as showed in Figure 4.10. Moreover, being ROOT libraries [46] provided inside the WBM framework, all the standard type of graphs, histograms and 2D map can be produced and specific algorithm, implemented in C++ scripting languages, can be run on.

4.3.2 Power System performances

The power system behavior is a crucial requirement to understand the detector response. During the last three years specific test campaigns on each single component have been performed to optimize the behavior of all the power distribution network elements (e.g. power supplies, cable, connectors), in order to stabilize the dark current response from the chambers and to minimize the external sources effects. From the power supply point of view, several are the improvements obtained during the commissioning phase both on the stability of the power supplies read-out and on the power distribution network grounding schema. After a long testing and optimization phase I carried out with CAEN engineers, a stable version of the HV board has been obtained, able to fulfill the RPC requirements

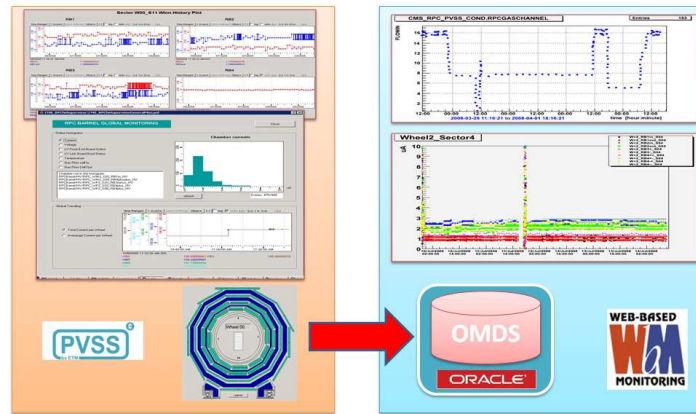


Figure 4.9. Data flow for the not event data acquired by PVSS. Data are stored in the online database and here analyzed by the CMS official database interface tools and then transmitted to the offline world.

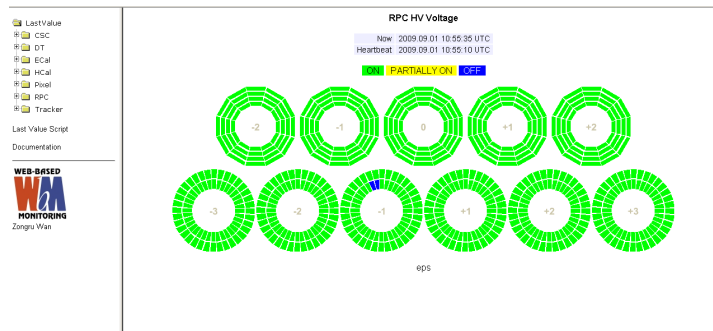
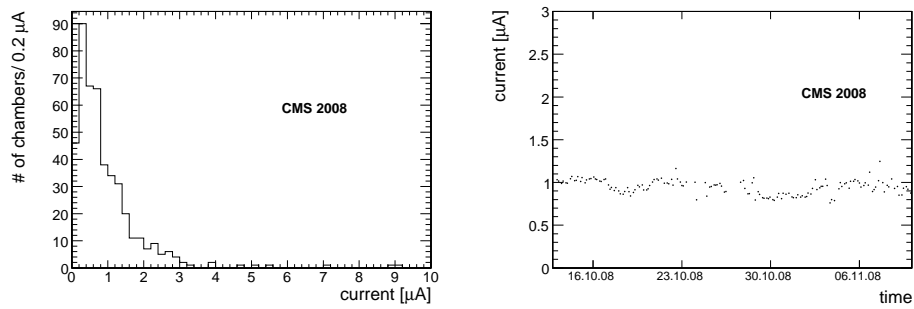


Figure 4.10. Typical GUI provided by the WBM framework to visualize the detector status from the stored data.



(a) Dark Current distribution at CRAFT end. The operating voltage is 9.2 kV.

(b) Average Dark current vs. time. The operating voltage is 9.2 kV.

Figure 4.11. RPC Current Behavior during CRAFT08.

in term of accuracy, offset stability and reliability in different operative conditions. The measured current is thus only depending on the chambers behavior and, as illustrated in the previous chapter, is highly affected by the variation of environmental conditions. The detector response from the dark current point of view has been matching the CMS requirements during the global runs. Figure 4.11a shows the dark current distribution at 9.2 kV for the 480 barrel chambers at the end of the CRAFT08 period. Fig. 4.11b shows its average value vs time. Very few chambers have values greater than $3 \mu\text{A}$ and the average has been almost stable around $1.5 \mu\text{A}$. No special correlation, at least on the mean values, has been found with the temperature variation in the explored range. On the LV system, the stability of supplied voltage has been reached with a acceptable ripple level of about 50-100 mV, ensuring the safe operation of the frontend chips and minimizing the external noise. The entire system in the final configuration has been working without any interruption since summer 2007, with a failure rate occurred less then 5%, and all the reparation has been realized without delaying the operation.

4.3.3 Temperature

The temperature has influence on the stability of the mechanical structures of the detector, on the response of the detecting elements, and on the electronics lifetime and safety. The global chamber operational temperature is highly correlated with the cooling system efficiency and stability. During the commissioning phase tests on the thermal environmental map have been performed in order to find out the environmental conditions with all the subsystems on and to spot hottest regions due to specific hardware configurations. The cooling system was evaluated and the results showed a good general operation stability. Special effort has been dedicated during the shut down period to increase the cooling circuit capability, reaching a very stable and satisfactory working situation and keeping all the chambers below the safety detector working threshold. In Figure 4.12 can be seen the dependency of the chambers and electronics temperature versus the cooling temperature on a reference chamber. Figure 4.13a and Figure 4.13b show the temperature distribution after a long data taking period and its average versus time. The system temperature is almost stable but when all the CMS electronics is switched on or off, a clear variation is visible.

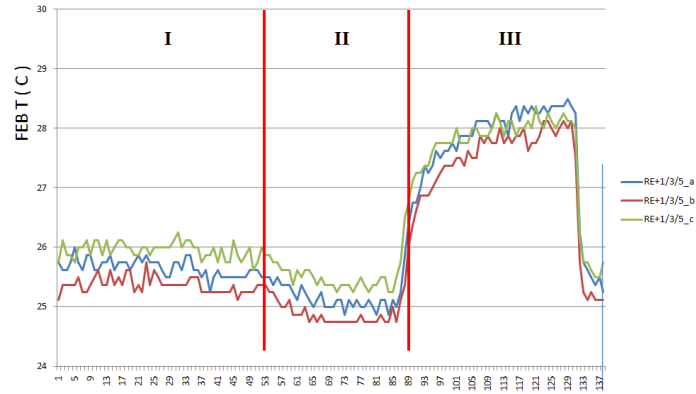
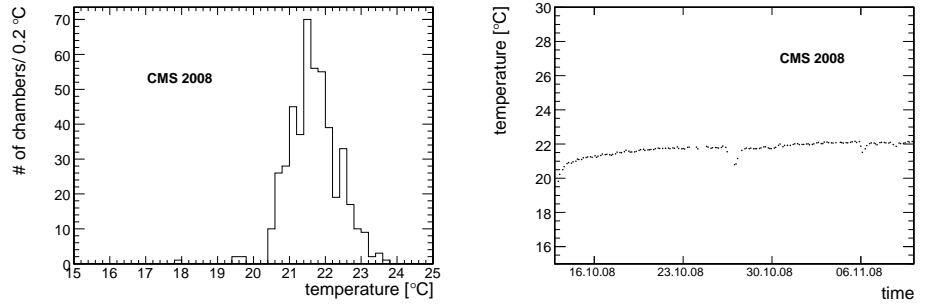


Figure 4.12. Typical dependency of the FEB temperature from the coolant temperature on some installed chambers. In the region **I** the stable working condition with cooling input water temperature at 20°C. In region **II** the input cooling water temperature was decreased to 19°C. In region **III** the chamber was temporarily excluded by the cooling circuit.



(a) RPC temperature distribution as measured by the probes installed inside the chambers. Measurements were taken at the end of the CRAFT period and are the average over one full day.

(b) Average RPC temperature vs time. The temperature variation is mainly due to the switching on or off of the CMS electronics.

Figure 4.13. Barrel Temperature behaviour during CRAFT08.

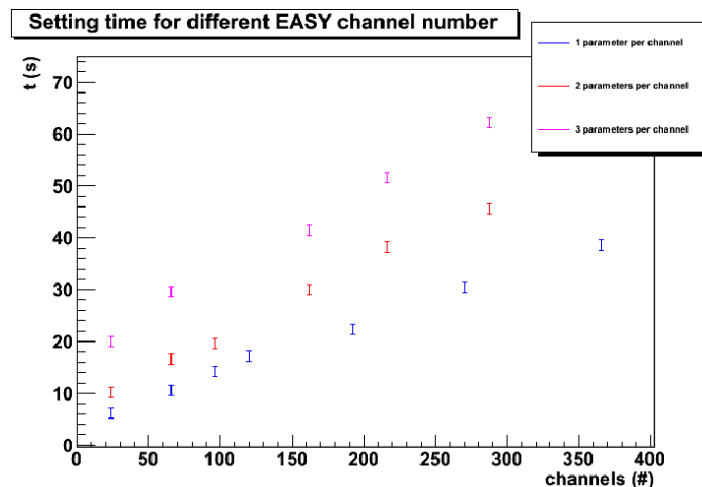


Figure 4.14. Time required to set different parameters for an increasing number of CAEN channels using PVSS and CAEN OPC Server 3.0. This configuration is representative of the max loads configuration used per SY1527 in our configuration.

4.3.4 DCS performances

The RCS was extensively tested during both the hardware installation phase and global data taking periods. After a short debug phase, the system ran without problems for the entire test period and showed that the architecture of the system met the requirements in speed, configurability and scalability. The DCS proved to be a reliable tool for the safe and correct operation of the detectors and trained shifter, were able to operate the detector in a easy and safe way. It was proved to be able to manage properly the interruptions occurred, due to power failures and communication problem with the power supplies, and to keep the detector in safe condition. The developed FSM adequately followed the detector's behavior and never lost control of the hardware.

The communication and the power supply control performances can be discussed in terms of the switching on/off speed and percentage of commands transmitted and lost. From the software point of view, the entire system is described by more then 20000 parameters, acquired from the hardware at about 100 Mb/hour. The communication with the CAEN power system is managed through the OPC protocol [36] and the software applications are distributed over four servers for resources optimization and loads balancing. The OPC server used, developed by CAEN, is the “CAEN OPC server”, version 3.0, where the acquisition is based on an event-driven approach. Studies of the powering of the system,

network load and performance have been performed for different settings and refresh speeds. The results of this test have allowed to identify bottle-necks in the system and have led to a better distribution of the work load among the different groups in the OPC Client side. In the best configuration achieved, the most significant parameters are handled with a 2 s refresh time and an average load per pc of about 5000 items, distributed over several OPC groups. Several studies on timing performance were performed with an increasing number of hardware channels using this OPC server/client configuration and showed a reasonable and effective behavior in the switching and setting operations (Fig. 4.14). Hence the time required during the switching on operation to bring the detector from OFF to ON state has been calculated to be about 470 s, mainly due to the detector mode operation.

Regarding the database performances, the communication with databases was worked stable and reliable along all the period. Data for the configuration are acquired from db and transmitted to the hardware in about 70 seconds, depending on the database load. The communication with the condition database has been working stably with high efficiency storage (less than $<0.3\%$ of data lost in the last year) and with optimized deadband. About 4 GBytes of Condition data was collected and stored in the CMS condition database at a storing rate of 30 Mbytes/day, reaching with optimized deadband a prescale factor of about 400 respect to data acquired.

Chapter 5

CONCLUSIONS

This thesis work was carried out in the frame of the Detector Control System (DCS) project of the CMS experiment at the CERN LHC collider. This thesis focuses on the control and monitoring of the RPC detector and all the auxiliary systems involved in the detector operation. The analysis of the requirements and project challenges, the architecture design and its development as well as the calibration and commissioning phases represent the main tasks developed for this PhD thesis work. It has required a deep knowledge of the different RPC subsystems (detector, readout, front end electronic and environmental conditions), and their behavior during the different working phases. Different technologies, middleware and solutions has been studied and adopted in the design and development of the different components and a big challenging consisted in the integration of these different parts each other and in the general CMS control system and data acquisition framework. I have been following this project from the beginning, as main responsible for the CMS RPC Group, along all the operative phases and now a stable version of the system is operative and used by the RPC collaboration.

The RPC DCS (RCS) is aimed to assure a continuous control and monitoring of the detector, the trigger and all the ancillary sub-systems (high voltages, low voltages, environmental, gas, and cooling), required to achieve the operational stability and reliability of a so large and complex detector and trigger system. It also takes appropriate corrective actions to maintain the detector stability and ensure high quality data, providing also an adequate user interfaces for experts or simple shifters. The working environment represents as well a challenge for the control system because of the high-radiation and magnetic fields environment. Therefore, the control system must be fault-tolerant and allow remote

diagnostics. As many functions of the RCS are needed at all time, the technologies and solutions adopted must ensure a 24/7 functioning for the entire life of the experiment.

From the hardware point of view, to reduce the design work, to ease commissioning and to minimize the maintenance effort required, commercial components have been selected in the system design wherever possible. The work in this thesis has led to the selection of components and technologies and to their validation in real cases. A crucial task carried out during this period has been the validation, the installation and the commissioning of the power supply system. After a long testing and optimization phase carried out with CAEN engineers, a stable version of the hardware has been obtained, able to fulfill the RPC requirements in term of accuracy, offset stability and reliability in different operative conditions. It has been delivered, installed and tested intensively in CMS during the last three years. Other crucial task has been the validation of the environmental system in term of stability and efficiency in the operation. During the commissioning phase tests on the thermal environmental map have been performed in order to find out the environmental condition with all the subsystems on and to spot hottest regions due to specific hardware configurations. The cooling system was also evaluated, showing a good general operation stability. Special effort has been dedicated to increase the cooling circuit capability, reaching a very stable and satisfactory working situation and keeping all the chambers below the safety detector working threshold. It was also demonstrated that the DSS system provided a satisfactory protection for the detector. The functionality of the independent hardware interlock were proven on several occasions protecting the detector modules from critical hazards conditions.

Concerning software, I have designed and developed the entire back end applications for monitoring the RPC detector operation, using the SCADA solution, PVSS, chosen by CERN for all the LHC experiments control systems. PVSS has been proven to be a suitable choice for the RPC requirements, able to provide the readout interfaces for various types of front end equipment, the possibility to store conditions data persistently in relational databases, the open design allowing for custom software extensions, and the good scalability within a highly distributed system. Additional features and further synergy effects in software development were achieved successfully thanks to the usage of the JCOP framework, developed by CERN IT/CO department to fulfill the common requirements of the four LHC experiments. All the control subsystems are able to work as stand-alone component and to participate the general RPC system operation, each covering a particular task. A RPC Supervisor level has also been design to gather all the information from all the subsystem involved in the rpc operation and to present a simplified but coherent and homogeneous interface to the operators. The main aim of the RPC Supervisor is to

summarize the status of all the sub-systems and present it to the central DCS, defining the operative conditions for data taking. It has been developed following the guidelines of the DCS central group, was proved to be reliable and stable, able to drive the detector behavior during all operative phases. It is demonstrated to be a useful tool for a prompt detector physics analysis and a powerful tool to prevent serious damages. It uses most of the functionalities provided by the JCOP+PVSS software, such as the finite state machine, the graphical user interface, the alarm handler and the ORACLE database interface, that allows the storage of the data in the CMS online database and the loading of the hardware configuration from the CMS configuration database. The RCS is operative since summer 2007 and running on a small farm of 6 PCs inside the CMS experiment. The entire project has been proved to respect all the CMS DCS guidelines and was successfully integrated in the CMS DCS during the summer 2007.

The commissioning run has been also used as system benchmarks and the DCS performance matched the challenging requirements as reported. The calibration procedures have been tested in the CMS environment and the performance has fulfilled the requirements. During the running-in phase it has been studied and analyzed the behavior of the Controls system under normal stable operational conditions as well as under abnormal and critical phases such as start-up, beam filling, magnet ramping, power outage, etc. in order to identify weak parts or bottlenecks of the system. Furthermore, the RCS allow studying the detector performance and adjusting the detector operation parameters to obtain the best detector response. This thesis has shown the importance of the RCS for CMS because of the complexity of the experiment and the large diversity of components utilized. The commissioning and validation of the RPC detector control system are now finished and it is currently running in the operational phase. The work presented here has contributed to the fully commissioning of the RPC detector and its calibration.

REFERENCES

- [1] M. Benedikt, P. Collier, V. Mertens, J. Poole, and K. Schindl. *LHC Design Report*. CERN, Geneva, 2004.
- [2] The ATLAS Collaboration. The atlas experiment at the cern large hadron collider. *Journal of Instrumentation*, 3(08):S08003, 2008.
- [3] The ALICE Collaboration and K Aamodt et al. The alice experiment at the cern lh. *Journal of Instrumentation*, 3(08):S08002, 2008.
- [4] CMS Collaboration. *CMS physics: Technical Design Report*. Technical Design Report CMS. CERN, Geneva, 2006. Detector performances.
- [5] The LHCb Collaboration and A Augusto Alves Jr et al. The lhcb detector at the lh. *Journal of Instrumentation*, 3(08):S08005, 2008.
- [6] Barate, R. et al. Search for the standard model Higgs boson at LEP. *Phys. Lett.*, B565:61–75, 2003.
- [7] G. Altarelli and Martin W. Grunewald. Precision electroweak tests of the standard model. *Phys. Rept.*, 403-404:189–201, 2004.
- [8] The TEVNPH Working Group. Combined CDF and D0 Upper Limits on Standard Model Higgs- Boson Production with up to 2.4 fb^{-1} of data. *arXiv*, 2008.
- [9] CMS Collaboration. *CMS physics: Technical Design Report*. Technical Design Report CMS. CERN, Geneva, 2006. Physics performaces.
- [10] V. Karimäki. *The CMS tracker system project: Technical Design Report*. Technical Design Report CMS. CERN, Geneva, 1997.
- [11] CMS Collaboration. *The CMS tracker: addendum to the Technical Design Report*. Technical Design Report CMS. CERN, Geneva, 2000.

- [12] CMS Collaboration. *The CMS electromagnetic calorimeter project: Technical Design Report*. Technical Design Report CMS. CERN, Geneva, 1997.
- [13] CMS Collaboration. *The CMS hadron calorimeter project: Technical Design Report*. Technical Design Report CMS. CERN, Geneva, 1997.
- [14] CMS Collaboration. *The CMS magnet project: Technical Design Report*. Technical Design Report CMS. CERN, Geneva, 1997.
- [15] CMS Collaboration. *The CMS muon project: Technical Design Report*. Technical Design Report CMS. CERN, Geneva, 1997.
- [16] CMS Collaboration. *CMS trigger and data-acquisition project: Technical Design Report*. Technical Design Report CMS. CERN, Geneva, 2002.
- [17] CMS Collaboration. *CMS TriDAS project: Technical Design Report; 1, the trigger systems*. Technical Design Report CMS.
- [18] B. G. Taylor. Timing distribution at the LHC. Prepared for 8th Workshop on Electronics for LHC Experiments, Colmar, France, 9-13 Sep 2002.
- [19] Brigljevic, V. et al. Using xdaq in application scenarios of the cms experiment. Technical Report CMS-CR-2003-007, CERN, Geneva, May 2003.
- [20] Box, D. et al. *Simple Object Access Protocol (SOAP) 1:1, W3C Note 08*. <http://www.w3.org/TR/SOAP>.
- [21] *For the I2O standard*. <http://developer.osdl.org/dev/opendoc/Online/Local/I20/index.html>.
- [22] Bauer, Gerry et al. The run control and monitoring system of the CMS experiment. *PoS, ACAT:026*, 2007.
- [23] I. Magrans de Arbril, E. Wulz, and J. Varela. Conceptual design of the cms trigger supervisor. *IEEE Trans. Nucl. Sci.*, 53:474–483, 2006.
- [24] Apache. *Axis is an XML based Web service framework*. <http://ws.apache.org/axis/>.
- [25] *The Apache Tomcat servlet container*. <http://tomcat.apache.org>.
- [26] Arcidiacono, R. et al. CMS DCS design concepts. *Conf. Proc.*, C051010:PO1.062–6, 2005.

- [27] *ETM professional control: PVSS (Prozess Visualisierung und Steuerungs System) SCADA tool*. <http://itcobe.web.cern.ch/itcobe/Services/Pvss/welcome.html>.
- [28] M. Gonzalez-Berges. The joint controls project framework. 2003.
- [29] B. Franek and C. Gaspar. SMI++: Object oriented framework for designing and implementing distributed control systems. Presented at 2004 IEEE Nuclear Science Symposium and Medical Imaging Conference (NSS / MIC), Rome, Italy, 16-22 Oct 2004.
- [30] P. Paolucci and G. Polese. The detector control systems for the cms resistive plate chamber. Technical Report CERN-CMS-NOTE-2008-036, CERN, Geneva, Apr 2008.
- [31] Abbrescia, M. et al. The gas monitoring system for the Resistive Plate Chamber detector of the CMS experiment at LHC. *Nuclear Physics B Proceedings Supplements*, 177:293–296, March 2008.
- [32] Abbrescia, M. et al. Performance of resistive plate chambers for the muon detection at CMS. *Nucl. Phys. Proc. Suppl.*, 78:90–95, 1999.
- [33] Abbrescia, M. et al. New developments on front end electronics for the CMS Resistive Plate Chambers. *Nucl. Instrum. Meth.*, A456:143–149, 2000.
- [34] Bunkowski, K. et al. Pattern comparator trigger algorithm: implementation in FPGA. In R. S. Romaniuk and K. T. Pozniak, editors, *Society of Photo-Optical Instrumentation Engineers (SPIE) Conference Series*, volume 5125 of *Society of Photo-Optical Instrumentation Engineers (SPIE) Conference Series*, pages 165–174, October 2003.
- [35] *CAN in Automation*. <http://www.can-cia.org/>.
- [36] *OPC Foundation*. <http://www.opcfoundation.org>.
- [37] Bunkowski, K. et al. Radiation tests of cms rpc muon trigger electronic components. *Nucl. Instrum. Meth.*, A538:708–717, 2005.
- [38] *CAEN S.p.A. Costruzioni Apparecchiature Elettroniche Nucleari*,. http://www.caen.it/nuclear/easy_info.php.
- [39] Aielli, G. et al. RPC operation at high temperature. *Nuclear Instruments and Methods in Physics Research A*, 508:44–49, August 2003.

- [40] Barillère, R. et al. Lhc gcs: A homogeneous approach for the control of the lhc experiments gas systems. 2003.
- [41] Abbrescia, M. et al. Results about HF production and bakelite analysis for the CMS Resistive Plate Chambers. *Nucl. Instrum. Meth.*, A594:140–147, 2008.
- [42] Benussi, L. et al. The CMS RPC gas gain monitoring system: an overview and preliminary results. *Nucl. Instrum. Meth.*, A602:805–808, 2009.
- [43] Adolphi, R. et al. The CMS experiment at the CERN LHC. *JINST*, 0803:S08004, 2008.
- [44] Colaleo, A. et al. First measurements of the performance of the Barrel RPC system in CMS. *Nuclear Instruments and Methods in Physics Research Section A: Accelerators, Spectrometers, Detectors and Associated Equipment*, 609(2-3):114 – 121, 2009.
- [45] *Web Based Monitoring*. <http://cmswbm.web.cern.ch/>.
- [46] R. Brun, F. Rademakers, and S. Panacek. Root, an object oriented data analysis framework. 2000.
- [47] G. Polese. The detector control systems for the cms resistive plate chamber. In *Nuclear Science Symposium Conference Record, 2008. NSS '08. IEEE*, pages 3228–3232, Oct. 2008.
- [48] P. Paolucci, G. Polese, R. Gómez-Reino, C. Viviani, R. Shahzad, and T. Khurshid. The detector control systems for the cms resistive plate chamber. Technical Report CERN-CMS-CR-2009-136, CERN, Geneva, May 2009.